

## Triplet-quadruplet dark matter

Tim M.P. Tait<sup>a</sup> and Zhao-Huan Yu<sup>a,b,c</sup>

<sup>a</sup>*Department of Physics and Astronomy, University of California,  
4129 Frederick Reines Hall, Irvine, California 92697, U.S.A.*

<sup>b</sup>*Key Laboratory of Particle Astrophysics,  
Institute of High Energy Physics, Chinese Academy of Sciences,  
19B Yuquan Road, Beijing 100049, China*

<sup>c</sup>*ARC Centre of Excellence for Particle Physics at the Terascale,  
School of Physics, The University of Melbourne,  
Tin Alley, Melbourne, Victoria 3010, Australia*

*E-mail:* [ttait@uci.edu](mailto:ttait@uci.edu), [zhao-huan.yu@unimelb.edu.au](mailto:zhao-huan.yu@unimelb.edu.au)

**ABSTRACT:** We explore a dark matter model extending the standard model particle content by one fermionic  $SU(2)_L$  triplet and two fermionic  $SU(2)_L$  quadruplets, leading to a minimal realistic UV-complete model of electroweakly interacting dark matter which interacts with the Higgs doublet at tree level via two kinds of Yukawa couplings. After electroweak symmetry-breaking, the physical spectrum of the dark sector consists of three Majorana fermions, three singly charged fermions, and one doubly charged fermion, with the lightest neutral fermion  $\chi_1^0$  serving as a dark matter candidate. A typical spectrum exhibits a large degree of degeneracy in mass between the neutral and charged fermions, and we examine the one-loop corrections to the mass differences to ensure that the lightest particle is neutral. We identify regions of parameter space for which the dark matter abundance is saturated for a standard cosmology, including coannihilation channels, and find that this is typically achieved for  $m_{\chi_1^0} \sim 2.4$  TeV. Constraints from precision electroweak measurements, searches for dark matter scattering with nuclei, and dark matter annihilation are important, but leave open a viable range for a thermal relic.

**KEYWORDS:** Beyond Standard Model, Cosmology of Theories beyond the SM

ARXIV EPRINT: [1601.01354](https://arxiv.org/abs/1601.01354)

---

**Contents**

<b>1</b>	<b>Introduction</b>	<b>1</b>
<b>2</b>	<b>Triplet-quadruplet dark matter</b>	<b>3</b>
<b>3</b>	<b>Custodial symmetry</b>	<b>6</b>
3.1	$m_Q < m_T$	6
3.2	$m_Q > m_T$	7
<b>4</b>	<b>One loop mass corrections</b>	<b>8</b>
<b>5</b>	<b>Constraints and relic density</b>	<b>10</b>
5.1	Relic abundance	12
5.2	Precision electroweak constraints	13
5.3	Scattering with heavy nuclei	13
5.4	Dark matter annihilation	15
5.5	Constraints on the $y_1$ - $y_2$ plane	15
<b>6</b>	<b>Conclusions and outlook</b>	<b>15</b>
<b>A</b>	<b>Detailed expressions for interaction terms</b>	<b>17</b>
<b>B</b>	<b>Self energies</b>	<b>21</b>

---

**1 Introduction**

With the discovery of the  $\sim 125$  GeV Higgs boson at the LHC [1, 2], the Standard Model (SM) of particle physics has been proven to be a self-consistent  $SU(3)_C \times SU(2)_L \times U(1)_Y$  gauge theory describing the strong and electroweak interactions of three generation quarks and leptons. However, the SM fails to describe astrophysical and cosmological observations, which are best explained by the existence of a massive neutral species of particle — dark matter (DM) [3–5]. While a variety of DM candidates are provided by extensions of the SM, among the most attractive are weakly interacting massive particles (WIMPs), which have roughly weak interaction strength and masses of  $\mathcal{O}(\text{GeV})$ – $\mathcal{O}(\text{TeV})$ . If WIMPs were thermally produced in the early Universe, they could give a desired relic abundance consistent with observation.

WIMPs typically appear in popular extensions of the SM aimed at addressing its deficiencies, such as e.g. supersymmetric [6, 7] and extra dimensional models [8, 9]. However, the need for their existence is independent of deep theoretical questions and it behooves us to leave no stone unturned in exploring the full range of possibilities. It is further natural to explore dark sectors containing  $SU(2)_L$  multiplets, whose neutral components are

natural DM candidates and whose interactions suggest the correct relic density for weak scale masses. Within the broad class of such models, both theoretical considerations and experimental results (most importantly, the null results of searches for WIMP scattering with heavy nuclei) provide important constraints on the viable constructions.

In *minimal* dark matter [10], the dark sector consists of a single scalar or fermion in a non-trivial  $SU(2)_L$  representation. For even-dimensional  $SU(2)_L$  representations, non-zero hypercharge is required to engineer an electrically neutral component, and typically results in a large coupling to the  $Z$  boson, which is excluded by direct searches for dark matter [11]. Odd-dimensional  $SU(2)_L$  representations have much weaker constraints, and lead to thermal relics for masses in the range of a few TeV.

If the dark sector consists of more than one  $SU(2)_L$  representation, electroweak symmetry-breaking allows for mixing between them, resulting in a much richer theoretical landscape. If the dark matter is a fermion, tree level renormalizable couplings to the Standard Model Higgs are permitted provided there are  $SU(2)_L$  representations differing in dimensionality by one. Such theories provide a theoretical laboratory to explore the possibility that the dark matter communicates to the SM predominantly via exchange of the electroweak and Higgs bosons.<sup>1</sup> The minimal module consists of a single odd-dimensional  $SU(2)_L$  representation Weyl fermion together with a vector-like pair (such that anomalies cancel) of even-dimensional representations with an appropriate hypercharge. Two such constructions which have been previously considered are *singlet-doublet dark matter* [12–17] and *doublet-triplet* dark matter [17, 18]. Both of these sets look (in the appropriate limit) like subsets of the neutralino sector of the minimal supersymmetric standard model (MSSM), and share some of its phenomenology.

In this work we investigate a case which does not emerge simply as a limit of the MSSM, *triplet-quadruplet* dark matter, consisting of one Weyl  $SU(2)_L$  triplet with  $Y = 0$  and two Weyl quadruplets with  $Y = \pm 1/2$ . After electroweak symmetry-breaking, the mass eigenstates include three neutral Majorana fermions  $\chi_i^0$ , three singly charged fermions  $\chi_i^\pm$ , and one doubly charged fermion  $\chi^{\pm\pm}$ , leading to unique features in the phenomenology. After imposing a discrete  $Z_2$  symmetry, and choosing the lightest neutral fermion  $\chi_1^0$  to be lighter than its charged siblings, we arrive at an exotic theory of dark matter whose interactions are mediated by the electroweak and Higgs bosons.

As with the singlet-doublet and doublet-triplet constructions, this theory is described by four parameters encapsulating two gauge-invariant mass terms ( $m_T$  and  $m_Q$ ) and two different Yukawa interactions coupling them to the SM Higgs doublet ( $y_1$  and  $y_2$ ). The limit  $y_1 = y_2$  realizes an enhanced custodial global symmetry resulting in  $\chi_1^0$  decoupling (at tree level) from the  $Z$  and Higgs bosons (provided  $m_Q < m_T$ ), greatly weakening the bounds from direct searches. It further implies that  $\chi_1^0$  is degenerate in mass with one of the charged states (and sometimes  $\chi^{\pm\pm}$ ) at tree level. For small deviations from this limit, the degeneracy is mildly lifted, requiring inclusion of the one-loop corrections to reliably establish that the lightest dark sector fermion is neutral.

---

<sup>1</sup>In contrast, scalar dark matter can always couple to the Higgs via renormalizable quartic interactions. We restrict our discussion to the fermionic case, leaving exploration of scalar dark sectors for future work.

This paper is outlined as follows. In section 2 we describe triplet-quadruplet dark matter in detail and establish notation. In section 3 we discuss the interesting features in the custodial symmetry limit. In section 4 we compute the corrections to the mass splittings at the one-loop level. In section 5 we identify the regions of parameter space resulting in the correct thermal relic abundance for a standard cosmology (including coannihilation channels) as well as the constraints from the electroweak oblique parameters and from direct and indirect searches. Section 6 contains our conclusions and further discussions. Appendix A gives the explicit expressions for the interaction terms, while appendix B lists the self-energy expressions which are used in the calculations of the mass corrections and electroweak oblique parameters.

## 2 Triplet-quadruplet dark matter

The triplet-quadruplet dark sector consists of colorless Weyl fermions  $T$ ,  $Q_1$ , and  $Q_2$  transforming under  $(SU(2)_L, U(1)_Y)$  as  $(\mathbf{3}, 0)$ ,  $(\mathbf{4}, -1/2)$ , and  $(\mathbf{4}, +1/2)$ . We denote their components as:

$$T = \begin{pmatrix} T^+ \\ T^0 \\ T^- \end{pmatrix}, \quad Q_1 = \begin{pmatrix} Q_1^+ \\ Q_1^0 \\ Q_1^- \\ Q_1^{--} \end{pmatrix}, \quad Q_2 = \begin{pmatrix} Q_2^{++} \\ Q_2^+ \\ Q_2^0 \\ Q_2^- \end{pmatrix}. \quad (2.1)$$

The two quadruplets are assigned opposite hypercharges in order to cancel gauge anomalies. Gauge-invariant kinetic and mass terms for the triplet and the quadruplets are given by

$$\mathcal{L}_T = iT^\dagger \bar{\sigma}^\mu D_\mu T - \frac{1}{2}(m_T TT + \text{h.c.}) \quad (2.2)$$

and

$$\mathcal{L}_Q = iQ_1^\dagger \bar{\sigma}^\mu D_\mu Q_1 + iQ_2^\dagger \bar{\sigma}^\mu D_\mu Q_2 - (m_Q Q_1 Q_2 + \text{h.c.}), \quad (2.3)$$

which specify their interactions with electroweak gauge bosons. They also couple to the SM Higgs doublet  $H$  through Yukawa interactions

$$\mathcal{L}_{\text{HTQ}} = y_1 \varepsilon_{jl} (Q_1)_i^{jk} T_k^i H^l - y_2 (Q_2)_i^{jk} T_k^i H_j^\dagger + \text{h.c.}, \quad (2.4)$$

where we use the tensor notation (see e.g. ref. [19]) to write down the triplet and quadruplets with  $SU(2)_L$   $\mathbf{2}$  (upper) and  $\bar{\mathbf{2}}$  (lower) indices explicitly indicated. We further assume there is a  $Z_2$  symmetry under which dark sector fermions are odd while SM particles are even to forbid renormalizable operators  $TLH$  and nonrenormalizable operators such as  $TeHH$ ,  $Q_1 L^\dagger HH^\dagger$ , and  $Q_2 LHH^\dagger$  (where  $L$  is a lepton doublet and  $e$  is a charged lepton singlet), which would lead the lightest dark sector fermion to decay.

In decomposing the  $SU(2)$  components, a traceless tensor  $\mathcal{T}_j^i$  in the  $\mathbf{3}$  representation is constructed from a  $\mathbf{2}$ ,  $u^i$ , and a  $\bar{\mathbf{2}}$ ,  $v_i$ , as

$$\mathcal{T}_j^i = u^i v_j - \frac{1}{2} \delta_j^i u^k v_k, \quad (2.5)$$

whereas a  $\mathbf{4}$ ,  $\mathcal{Q}_k^{ij}$ , is constructed via

$$\mathcal{Q}_k^{ij} = \frac{1}{2} \left( \mathcal{T}_k^i u^j + \mathcal{T}_k^j u^i - \frac{1}{3} \delta_k^i \mathcal{T}_l^j u^l - \frac{1}{3} \delta_k^j \mathcal{T}_l^i u^l \right), \quad (2.6)$$

which is symmetric in the upper indices  $i$  and  $j$ , and satisfies  $\sum_k \mathcal{Q}_k^{kj} = \sum_k \mathcal{Q}_k^{ik} = 0$ . Taking into account the normalization of the Lagrangians (2.2) and (2.3), we can identify the components of  $T$ ,  $Q_1$ , and  $Q_2$  in the vector notation (2.1) with those in the tensor notation via:

$$T^+ = T_2^1, \quad T^0 = \sqrt{2}T_1^1 = -\sqrt{2}T_2^2, \quad T^- = T_1^2; \quad (2.7)$$

$$Q_1^+ = (Q_1)_2^{11}, \quad Q_1^0 = \sqrt{3}(Q_1)_1^{11} = -\sqrt{3}(Q_1)_2^{12} = -\sqrt{3}(Q_1)_2^{21}, \quad (2.8)$$

$$Q_1^- = \sqrt{3}(Q_1)_2^{22} = -\sqrt{3}(Q_1)_1^{12} = -\sqrt{3}(Q_1)_1^{21}, \quad Q_1^{-+} = (Q_1)_1^{22}; \quad (2.9)$$

$$Q_2^{++} = (Q_2)_2^{11}, \quad Q_2^+ = \sqrt{3}(Q_2)_1^{11} = -\sqrt{3}(Q_2)_2^{12} = -\sqrt{3}(Q_2)_2^{21}, \quad (2.10)$$

$$Q_2^0 = \sqrt{3}(Q_2)_2^{22} = -\sqrt{3}(Q_2)_1^{12} = -\sqrt{3}(Q_2)_1^{21}, \quad Q_2^- = (Q_2)_1^{22}. \quad (2.11)$$

Thus, the mass terms decompose into

$$-\frac{1}{2}m_T TT \equiv -\frac{1}{2}m_T T_i^j T_j^i = -m_T T^- T^+ - \frac{1}{2}m_T T^0 T^0 \quad (2.12)$$

and

$$-m_Q Q_1 Q_2 \equiv -m_Q \varepsilon_{il} (Q_1)_k^{ij} (Q_2)_j^{lk} = -m_Q (Q_1^{-+} Q_2^{++} - Q_1^- Q_2^+ + Q_1^0 Q_2^0 - Q_1^+ Q_2^-). \quad (2.13)$$

The explicit form of the Higgs doublet is

$$H^i = \begin{pmatrix} H^+ \\ H^0 \end{pmatrix}, \quad H_i^\dagger = (H^-, H^{0*}), \quad (2.14)$$

leading to

$$H^i(x) = \frac{1}{\sqrt{2}} \begin{pmatrix} 0 \\ v + h(x) \end{pmatrix} \quad (2.15)$$

after electroweak symmetry-breaking in the unitary gauge. Then

$$\begin{aligned} \mathcal{L}_{\text{HTQ}} \rightarrow & y_1 (v + h) \left( \frac{1}{\sqrt{6}} Q_1^- T^+ - \frac{1}{\sqrt{3}} Q_1^0 T^0 - \frac{1}{\sqrt{2}} Q_1^+ T^- \right) \\ & + y_2 (v + h) \left( \frac{1}{\sqrt{3}} Q_2^0 T^0 + \frac{1}{\sqrt{6}} Q_2^+ T^- - \frac{1}{\sqrt{2}} Q_2^- T^+ \right). \end{aligned} \quad (2.16)$$

The complete model-dependence is specified by the four parameters,

$$\{m_T, m_Q, y_1, y_2\}. \quad (2.17)$$

By choosing appropriate field redefinitions,  $m_T$ ,  $y_1$ , and  $y_2$  can be made to be real, such that the phase of  $m_Q$  is the only source of  $CP$  violation in the dark sector. However, here we do not consider  $CP$  violation effects and take all of them to be real. Moreover, taking

$m_T \rightarrow -m_T$ , the transformation  $m_Q \rightarrow -m_Q$  or  $y_2 \rightarrow -y_2$  each yields the same Lagrangian up to field redefinitions. Therefore, we consider  $m_T$  and  $m_Q$  both positive without loss of generality.

After electroweak symmetry breaking, the full set of mass terms can be written

$$\begin{aligned} \mathcal{L}_{\text{mass}} &= -m_Q Q_1^{--} Q_2^{++} - \frac{1}{2} (T^0, Q_1^0, Q_2^0) \mathcal{M}_N \begin{pmatrix} T^0 \\ Q_1^0 \\ Q_2^0 \end{pmatrix} - (T^-, Q_1^-, Q_2^-) \mathcal{M}_C \begin{pmatrix} T^+ \\ Q_1^+ \\ Q_2^+ \end{pmatrix} + \text{h.c.} \\ &= -m_Q \chi^{--} \chi^{++} - \frac{1}{2} \sum_{i=1}^3 m_{\chi_i^0} \chi_i^0 \chi_i^0 - \sum_{i=1}^3 m_{\chi_i^\pm} \chi_i^- \chi_i^+ + \text{h.c.}, \end{aligned} \quad (2.18)$$

where  $\chi^{--} \equiv Q_1^{--}$  and  $\chi^{++} \equiv Q_2^{++}$ . The mass matrices for the neutral and charged fermions are given by

$$\mathcal{M}_N = \begin{pmatrix} m_T & \frac{1}{\sqrt{3}} y_1 v & -\frac{1}{\sqrt{3}} y_2 v \\ \frac{1}{\sqrt{3}} y_1 v & 0 & m_Q \\ -\frac{1}{\sqrt{3}} y_2 v & m_Q & 0 \end{pmatrix}, \quad \mathcal{M}_C = \begin{pmatrix} m_T & \frac{1}{\sqrt{2}} y_1 v & -\frac{1}{\sqrt{6}} y_2 v \\ -\frac{1}{\sqrt{6}} y_1 v & 0 & -m_Q \\ \frac{1}{\sqrt{2}} y_2 v & -m_Q & 0 \end{pmatrix}. \quad (2.19)$$

They are diagonalized by three unitary matrices,  $\mathcal{N}$ ,  $\mathcal{C}_L$ , and  $\mathcal{C}_R$ :

$$\mathcal{N}^T \mathcal{M}_N \mathcal{N} = \tilde{\mathcal{M}}_N = \text{diag}(m_{\chi_1^0}, m_{\chi_2^0}, m_{\chi_3^0}), \quad (2.20)$$

$$\mathcal{C}_R^T \mathcal{M}_C \mathcal{C}_L = \tilde{\mathcal{M}}_C = \text{diag}(m_{\chi_1^\pm}, m_{\chi_2^\pm}, m_{\chi_3^\pm}), \quad (2.21)$$

with the gauge eigenstates related to the mass eigenstates by

$$\begin{pmatrix} T^0 \\ Q_1^0 \\ Q_2^0 \end{pmatrix} = \mathcal{N} \begin{pmatrix} \chi_1^0 \\ \chi_2^0 \\ \chi_3^0 \end{pmatrix}, \quad \begin{pmatrix} T^+ \\ Q_1^+ \\ Q_2^+ \end{pmatrix} = \mathcal{C}_L \begin{pmatrix} \chi_1^+ \\ \chi_2^+ \\ \chi_3^+ \end{pmatrix}, \quad \begin{pmatrix} T^- \\ Q_1^- \\ Q_2^- \end{pmatrix} = \mathcal{C}_R \begin{pmatrix} \chi_1^- \\ \chi_2^- \\ \chi_3^- \end{pmatrix}. \quad (2.22)$$

Therefore, the dark sector fermions consist of three Majorana fermions  $\chi_i^0$ , three singly charged fermions  $\chi_i^\pm$ , and one doubly charged fermion  $\chi^{\pm\pm}$ . Here we denote the particles in order of mass, i.e.,  $m_{\chi_1^0} \leq m_{\chi_2^0} \leq m_{\chi_3^0}$  and  $m_{\chi_1^\pm} \leq m_{\chi_2^\pm} \leq m_{\chi_3^\pm}$ . The lightest new particle is stable as a result of the imposed  $Z_2$  symmetry. Consequently, we identify parameters such that  $\chi_1^0$  is lighter than  $\chi_1^\pm$  and  $\chi^{\pm\pm}$ , in order for  $\chi_1^0$  to effectively play the role of dark matter.

We can construct 4-component fermionic fields from the Weyl fields:

$$X_i^0 = \begin{pmatrix} \chi_{iL}^0 \\ (\chi_{iR}^0)^\dagger \end{pmatrix}, \quad X_i^+ = \begin{pmatrix} \chi_{iL}^+ \\ (\chi_{iR}^-)^\dagger \end{pmatrix}, \quad X^{++} = \begin{pmatrix} \chi_L^{++} \\ (\chi_R^{--})^\dagger \end{pmatrix}, \quad (2.23)$$

where

$$\chi_L^0 = \chi_R^0 = (\chi_1^0, \chi_2^0, \chi_3^0)^T, \quad \chi_L^+ = (\chi_1^+, \chi_2^+, \chi_3^+)^T, \quad \chi_R^- = (\chi_1^-, \chi_2^-, \chi_3^-)^T, \quad (2.24)$$

$$\chi_L^{++} = \chi^{++}, \quad \chi_R^{--} = \chi^{--}. \quad (2.25)$$

And the mass basis is defined such that they have diagonal mass terms:

$$\mathcal{L}_{\text{mass}} = -m_Q \bar{X}^{++} X^{++} - \frac{1}{2} \sum_{i=1}^3 m_{\chi_i^0} \bar{X}_i^0 X_i^0 - \sum_{i=1}^3 m_{\chi_i^\pm} \bar{X}_i^\pm X_i^\pm. \quad (2.26)$$

### 3 Custodial symmetry

If  $y_1$  is equal to  $y_2$ , there exists a global custodial  $SU(2)_R$  global symmetry, as is well known in the SM Higgs sector. Under this symmetry the triplet is an  $SU(2)_R$  singlet, while the quadruplets and the Higgs field are both  $SU(2)_R$  doublets:

$$(\mathbf{Q}_A)_k^{ij} = \begin{pmatrix} (Q_1)_k^{ij} \\ (Q_2)_k^{ij} \end{pmatrix}, \quad (\mathbf{H}_A)_i = \begin{pmatrix} H_i^\dagger \\ H_i \end{pmatrix}, \quad (3.1)$$

where  $H_i \equiv \varepsilon_{ij} H^j$  and  $A$  is an  $SU(2)_R$  index.  $\mathcal{L}_Q$  and  $\mathcal{L}_{\text{HTQ}}$  can be expressed in an  $SU(2)_L \times SU(2)_R$  invariant form:

$$\begin{aligned} \mathcal{L}_Q + \mathcal{L}_{\text{HTQ}} &= i(\mathbf{Q}^{\dagger A})_k^{ij} \bar{\sigma}^\mu D_\mu (\mathbf{Q}_A)_k^{ij} - \frac{1}{2} m_Q \left[ \varepsilon^{AB} \varepsilon_{il} (\mathbf{Q}_A)_k^{ij} (\mathbf{Q}_B)_j^{lk} + \text{h.c.} \right] \\ &\quad + \left[ y \varepsilon^{AB} (\mathbf{Q}_A)_i^{jk} T_k^i (\mathbf{H}_B)_j + \text{h.c.} \right], \end{aligned} \quad (3.2)$$

where  $y = y_1 = y_2$ . This symmetry is also found in the singlet-doublet model [13–15] and the doublet-triplet model [18]. Though broken by the  $U(1)_Y$  gauge symmetry, nonetheless it dictates some tree level relations with important implications. We describe the cases  $m_Q < m_T$  and  $m_Q > m_T$  separately below.

#### 3.1 $m_Q < m_T$

If  $m_Q < m_T$ , the leading order (LO) dark sector fermion masses can be derived to be:

$$m_{\chi_1^0}^{\text{LO}} = m_{\chi_1^\pm}^{\text{LO}} = m_{\chi^{\pm\pm}}^{\text{LO}} = m_Q, \quad (3.3)$$

$$m_{\chi_2^0}^{\text{LO}} = m_{\chi_2^\pm}^{\text{LO}} = \frac{1}{2} \left[ \sqrt{8y^2 v^2 / 3 + (m_Q + m_T)^2} + m_Q - m_T \right], \quad (3.4)$$

$$m_{\chi_3^0}^{\text{LO}} = m_{\chi_3^\pm}^{\text{LO}} = \frac{1}{2} \left[ \sqrt{8y^2 v^2 / 3 + (m_Q + m_T)^2} - m_Q + m_T \right], \quad (3.5)$$

while the mixing matrices take the form

$$\mathcal{N} = \begin{pmatrix} 0 & \frac{ai}{b} & -\frac{\sqrt{2}}{b} \\ \frac{1}{\sqrt{2}} & -\frac{i}{b} & -\frac{a}{\sqrt{2}b} \\ \frac{1}{\sqrt{2}} & \frac{i}{b} & \frac{a}{\sqrt{2}b} \end{pmatrix}, \quad \mathcal{C}_L = \begin{pmatrix} 0 & \frac{a}{b} & -\frac{\sqrt{2}i}{b} \\ \frac{i}{2} & -\frac{\sqrt{6}}{2b} & -\frac{\sqrt{3}ai}{2b} \\ \frac{\sqrt{3}i}{2} & \frac{\sqrt{2}}{2b} & \frac{ai}{2b} \end{pmatrix}, \quad \mathcal{C}_R = \begin{pmatrix} 0 & -\frac{a}{b} & \frac{\sqrt{2}i}{b} \\ \frac{\sqrt{3}i}{2} & -\frac{\sqrt{2}}{2b} & -\frac{ai}{2b} \\ \frac{i}{2} & \frac{\sqrt{6}}{2b} & \frac{\sqrt{3}ai}{2b} \end{pmatrix}, \quad (3.6)$$

where

$$a \equiv \frac{\sqrt{8y^2 v^2 / 3 + (m_Q + m_T)^2} - m_Q - m_T}{2yv/\sqrt{3}} \quad \text{and} \quad b \equiv \sqrt{2 + a^2}. \quad (3.7)$$

Thus each of the neutral fermions is degenerate in mass with a singly charged fermion, and the lightest one is also degenerate with the doubly charged fermion, which always

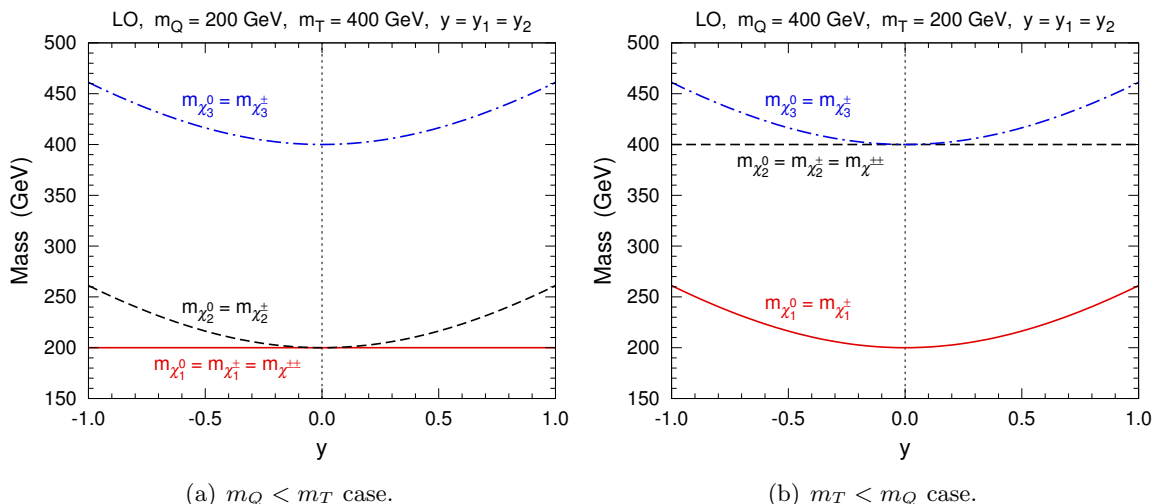


**Figure 1.** Fermion masses as functions of  $y$  in the custodial symmetry limit at LO. The left (right) panel corresponds to  $m_Q = 200$  (400) GeV and  $m_T = 400$  (200) GeV.

has a mass of  $m_Q$ . In figure 1(a), we show the mass spectrum for  $m_Q = 200$  GeV and  $m_T = 400$  GeV. If  $y = 0$ , the quadruplets would not mix with the triplet, and we would have  $m_{\chi_1^0}^{\text{LO}} = m_{\chi_1^\pm}^{\text{LO}} = m_{\chi_2^0}^{\text{LO}} = m_{\chi_2^\pm}^{\text{LO}} = m_{\chi^{\pm\pm}}^{\text{LO}} = m_Q$  and  $m_{\chi_3^0}^{\text{LO}} = m_{\chi_3^\pm}^{\text{LO}} = m_T$ . As  $|y|$  increases,  $\chi_2^0$ ,  $\chi_3^0$ ,  $\chi_2^\pm$ , and  $\chi_3^\pm$  become heavier. At loop level the custodial symmetry realizes that it is broken by  $U(1)_Y$ , and corrections from the loops of electroweak bosons lift the degeneracies [10, 20, 21]. We examine the next-to-leading (NLO) corrections to the masses in detail in section 4.

In general, the  $\chi_1^0$  couplings to the Higgs boson and to the  $Z$  boson are proportional to  $(y_1 \mathcal{N}_{21} - y_2 \mathcal{N}_{31}) \mathcal{N}_{11}$  and  $(|\mathcal{N}_{31}|^2 - |\mathcal{N}_{21}|^2)$ , respectively. In the custodial symmetry limit, the interaction properties of  $\chi_1^0$  are quite special. From the explicit expression of  $\mathcal{N}$  in eq. (3.6), we can find that there is no triplet component in  $\chi_1^0$  and  $\mathcal{N}_{21} = \mathcal{N}_{31} = 1/\sqrt{2}$ , i.e.,  $\chi_1^0 = (Q_1^0 + Q_2^0)/\sqrt{2}$ . Therefore, the  $\chi_1^0$  coupling to the Higgs boson vanishes because this coupling exists only when the  $T^0$  component is involved. Moreover, there is no  $\chi_1^0$  coupling to the  $Z$  boson, since  $Q_1^0$  and  $Q_2^0$  have opposite hypercharges and opposite eigenvalues of the third  $SU(2)_L$  generator. As a result,  $\chi_1^0$  cannot interact with nuclei at tree level and generically escapes from direct detection bounds.

### 3.2 $m_Q > m_T$

If  $m_Q > m_T$  and  $|yv| < \sqrt{3m_Q(m_Q - m_T)}$ , the fermion masses are

$$m_{\chi_1^0}^{\text{LO}} = m_{\chi_1^\pm}^{\text{LO}} = \frac{1}{2} \left[ \sqrt{8y^2v^2/3 + (m_Q + m_T)^2} - m_Q + m_T \right], \quad (3.8)$$

$$m_{\chi_2^0}^{\text{LO}} = m_{\chi_2^\pm}^{\text{LO}} = m_{\chi^{\pm\pm}}^{\text{LO}} = m_Q, \quad (3.9)$$

$$m_{\chi_3^0}^{\text{LO}} = m_{\chi_3^\pm}^{\text{LO}} = \frac{1}{2} \left[ \sqrt{8y^2v^2/3 + (m_Q + m_T)^2} + m_Q - m_T \right], \quad (3.10)$$

and  $\chi_1^0$  is a mixture of  $T^0$ ,  $Q_1^0$ , and  $Q_2^0$ :

$$\chi_1^0 = -\frac{i}{b}(aT^0 - Q_1^0 + Q_2^0). \quad (3.11)$$

In this case, the coupling to the Higgs boson does not vanish, that with the  $Z$  boson still vanishes because  $|\mathcal{N}_{21}|^2 = |\mathcal{N}_{31}|^2 = 1/b^2$ . Consequently,  $\chi_1^0$  can interact with nuclei through the Higgs exchange at tree level. Figure 1(b) shows the mass spectrum for  $m_Q = 400$  GeV and  $m_T = 200$  GeV.

If  $m_Q > m_T$  and  $|yv| > \sqrt{3m_Q(m_Q - m_T)}$ , we have

$$m_Q < \frac{1}{2} \left[ \sqrt{8y^2v^2/3 + (m_Q + m_T)^2} - m_Q + m_T \right],$$

and hence  $m_{\chi_1^0} = m_Q$  and  $\chi_1^0 = (Q_1^0 + Q_2^0)/\sqrt{2}$ , whose interactions are similar to the case of  $m_Q < m_T$  described above.

#### 4 One loop mass corrections

In this section, we calculate the dark fermion mass corrections at NLO, determining the parameter space for which  $\chi_1^0$  is lighter than  $\chi_1^\pm$  and  $\chi^{\pm\pm}$ .

For mixed fermionic fields  $X_i$  (either  $X_i^0$  or  $X_i^\pm$ ), renormalized one-particle irreducible two-point functions can be written down as [22, 23]

$$\begin{aligned} \hat{\Sigma}_{X_i X_j}(q) &= (\not{q} - m_{\chi_i})\delta_{ij} + \Sigma_{X_i X_j}(q) - \delta\tilde{\mathcal{M}}_{ij}P_L - \delta\tilde{\mathcal{M}}_{ji}^*P_R \\ &+ \frac{1}{2}(\not{q} - m_{\chi_i})(\delta Z_{ij}^L P_L + \delta Z_{ij}^{R*} P_R) + \frac{1}{2}(\delta Z_{ji}^{L*} P_R + \delta Z_{ji}^R P_L)(\not{q} - m_{\chi_j}), \end{aligned} \quad (4.1)$$

where  $P_L \equiv \frac{1}{2}(1 - \gamma_5)$  and  $P_R \equiv \frac{1}{2}(1 + \gamma_5)$  are chiral projectors and  $\delta\tilde{\mathcal{M}}_{ij}$  are mass renormalization constants defined by  $\tilde{\mathcal{M}}_{ij,0} = \tilde{\mathcal{M}}_{ij} + \delta\tilde{\mathcal{M}}_{ij}$ , where the subscript 0 denotes a bare quantity and the diagonalized mass matrix  $\tilde{\mathcal{M}}$  stands for either  $\tilde{\mathcal{M}}_N$  or  $\tilde{\mathcal{M}}_C$ . The wave function renormalization constants  $\delta Z_{ij}^L$  and  $\delta Z_{ij}^R$  are defined as  $X_{i,0} = X_i + \frac{1}{2}(\delta Z_{ij}^L P_L + \delta Z_{ij}^{R*} P_R)X_j$ . The self-energy  $\Sigma_{X_i X_j}(q)$  can be decomposed into Lorentz structures:

$$\Sigma_{X_i X_j}(q) = P_L \Sigma_{X_i X_j}^{\text{LS}}(q^2) + P_R \Sigma_{X_i X_j}^{\text{RS}}(q^2) + \not{q} P_L \Sigma_{X_i X_j}^{\text{LV}}(q^2) + \not{q} P_R \Sigma_{X_i X_j}^{\text{RV}}(q^2), \quad (4.2)$$

and Hermiticity relates these functions:

$$\Sigma_{X_i X_j}^{\text{RS}}(q^2) = \Sigma_{X_j X_i}^{\text{LS}*}(q^2), \quad \Sigma_{X_i X_j}^{\text{LV}}(q^2) = \Sigma_{X_j X_i}^{\text{LV}*}(q^2), \quad \Sigma_{X_i X_j}^{\text{RV}}(q^2) = \Sigma_{X_j X_i}^{\text{RV}*}(q^2). \quad (4.3)$$

There are additional constraints for Majorana fields  $X_i^0$ :

$$\Sigma_{X_i^0 X_j^0}^{\text{LS}}(q^2) = \Sigma_{X_j^0 X_i^0}^{\text{LS}}(q^2), \quad \Sigma_{X_i^0 X_j^0}^{\text{RS}}(q^2) = \Sigma_{X_j^0 X_i^0}^{\text{RS}}(q^2), \quad \Sigma_{X_i^0 X_j^0}^{\text{LV}}(q^2) = \Sigma_{X_j^0 X_i^0}^{\text{RV}}(q^2), \quad (4.4)$$

which we utilize as a cross-check on our calculations.

On-shell, there should be no mixing between states in the mass basis. Using the definition of the pole mass in the on-shell scheme leads to the renormalization condition:

$$\widetilde{\text{Re}} \hat{\Sigma}_{X_i X_j}(q) u_{X_j}(q) = 0 \quad \text{for } q^2 = m_{\chi_j}^2, \quad (4.5)$$

where  $\widetilde{\text{Re}}$  takes the real parts of the loop integrals in self-energies but leaves the couplings intact. This condition fixes the mass renormalization constants to

$$\delta\tilde{\mathcal{M}}_{ij} = \frac{1}{2}\widetilde{\text{Re}} \left[ \Sigma_{X_i X_j}^{\text{LS}}(m_{\chi_i}^2) + \Sigma_{X_i X_j}^{\text{LS}}(m_{\chi_j}^2) + m_{\chi_i} \Sigma_{X_i X_j}^{\text{LV}}(m_{\chi_i}^2) + m_{\chi_j} \Sigma_{X_i X_j}^{\text{RV}}(m_{\chi_j}^2) \right]. \quad (4.6)$$

As in refs. [22, 24] for the renormalization of neutralinos and charginos, we introduce renormalization constants  $\delta\mathcal{M}_N$  and  $\delta\mathcal{M}_C$  to shift the mass matrices  $\mathcal{M}_N$  and  $\mathcal{M}_C$ , but the mixing matrices  $\mathcal{N}$ ,  $\mathcal{C}_L$ , and  $\mathcal{C}_R$  remain the same at NLO as at LO. Therefore, we have

$$(\delta\mathcal{M}_N)_{ij} = (\mathcal{N}^* \delta\tilde{\mathcal{M}}_N \mathcal{N}^\dagger)_{ij} = \mathcal{N}_{ik}^* \mathcal{N}_{jl}^* (\delta\tilde{\mathcal{M}}_N)_{kl}, \quad (4.7)$$

and

$$(\delta\tilde{\mathcal{M}}_C)_{ij} = (\mathcal{C}_R^\text{T} \delta\mathcal{M}_C \mathcal{C}_L)_{ij} = (\mathcal{C}_R)_{ki} (\mathcal{C}_L)_{lj} (\delta\mathcal{M}_C)_{kl}. \quad (4.8)$$

Furthermore, we choose to renormalize the Majorana fermion masses on-shell, i.e.,

$$m_{\chi_i^0}^{\text{NLO}} = m_{\chi_i^0}, \quad (4.9)$$

and compute the relative shifts in the masses of  $\chi_i^\pm$  and  $\chi^{\pm\pm}$ . In this scheme eq. (4.7) provides the NLO shifts in the parameters  $m_T$ ,  $m_Q$ ,  $y_1$ , and  $y_2$ :

$$\delta m_T = \mathcal{N}_{1k}^* \mathcal{N}_{1l}^* (\delta\tilde{\mathcal{M}}_N)_{kl}, \quad \delta m_Q = \mathcal{N}_{2k}^* \mathcal{N}_{3l}^* (\delta\tilde{\mathcal{M}}_N)_{kl}, \quad (4.10)$$

$$v\delta y_1 = \sqrt{3} \mathcal{N}_{1k}^* \mathcal{N}_{2l}^* (\delta\tilde{\mathcal{M}}_N)_{kl}, \quad v\delta y_2 = -\sqrt{3} \mathcal{N}_{1k}^* \mathcal{N}_{3l}^* (\delta\tilde{\mathcal{M}}_N)_{kl}, \quad (4.11)$$

where  $\delta\tilde{\mathcal{M}}_N$  is given by eq. (4.6):

$$(\delta\tilde{\mathcal{M}}_N)_{ij} = \frac{1}{2}\widetilde{\text{Re}} \left[ \Sigma_{X_i^0 X_j^0}^{\text{LS}}(m_{\chi_i^0}^2) + \Sigma_{X_i^0 X_j^0}^{\text{LS}}(m_{\chi_j^0}^2) + m_{\chi_i^0} \Sigma_{X_i^0 X_j^0}^{\text{LV}}(m_{\chi_i^0}^2) + m_{\chi_j^0} \Sigma_{X_i^0 X_j^0}^{\text{RV}}(m_{\chi_j^0}^2) \right]. \quad (4.12)$$

The shifts on these parameters shift  $\tilde{\mathcal{M}}_C$  through eq. (4.8). As a result, the physical masses of  $\chi_i^\pm$  at NLO are given by

$$m_{\chi_i^\pm}^{\text{NLO}} = m_{\chi_i^\pm} + (\delta\tilde{\mathcal{M}}_C)_{ii} - \frac{1}{2}\widetilde{\text{Re}} \left\{ 2\Sigma_{X_i^+ X_i^+}^{\text{LS}}(m_{\chi_i^\pm}^2) + m_{\chi_i^\pm} \left[ \Sigma_{X_i^+ X_i^+}^{\text{LV}}(m_{\chi_i^\pm}^2) + \Sigma_{X_i^+ X_i^+}^{\text{RV}}(m_{\chi_i^\pm}^2) \right] \right\}, \quad (4.13)$$

where

$$\begin{aligned} (\delta\tilde{\mathcal{M}}_C)_{ii} &= \sum_{jk} (\mathcal{C}_R)_{ji} (\mathcal{C}_L)_{ki} (\delta\mathcal{M}_C)_{jk} \\ &= - \left[ (\mathcal{C}_R)_{2i} (\mathcal{C}_L)_{3i} + (\mathcal{C}_R)_{3i} (\mathcal{C}_L)_{2i} \right] \delta m_Q + \frac{1}{\sqrt{6}} v \delta y_1 \left[ \sqrt{3} (\mathcal{C}_R)_{1i} (\mathcal{C}_L)_{2i} - (\mathcal{C}_R)_{2i} (\mathcal{C}_L)_{1i} \right] \\ &\quad + (\mathcal{C}_R)_{1i} (\mathcal{C}_L)_{1i} \delta m_T + \frac{1}{\sqrt{6}} v \delta y_2 \left[ \sqrt{3} (\mathcal{C}_R)_{3i} (\mathcal{C}_L)_{1i} - (\mathcal{C}_R)_{1i} (\mathcal{C}_L)_{3i} \right]. \end{aligned} \quad (4.14)$$

The physical mass of  $\chi^{\pm\pm}$  is affected by the shift in  $m_Q$ :

$$\begin{aligned} m_{\chi^{\pm\pm}}^{\text{NLO}} &= m_Q + \delta m_Q - \frac{1}{2}\widetilde{\text{Re}} \left\{ 2\Sigma_{X^{++} X^{++}}^{\text{LS}}(m_{\chi^{\pm\pm}}^2) \right. \\ &\quad \left. + m_Q \left[ \Sigma_{X^{++} X^{++}}^{\text{LV}}(m_{\chi^{\pm\pm}}^2) + \Sigma_{X^{++} X^{++}}^{\text{RV}}(m_{\chi^{\pm\pm}}^2) \right] \right\}. \end{aligned} \quad (4.15)$$

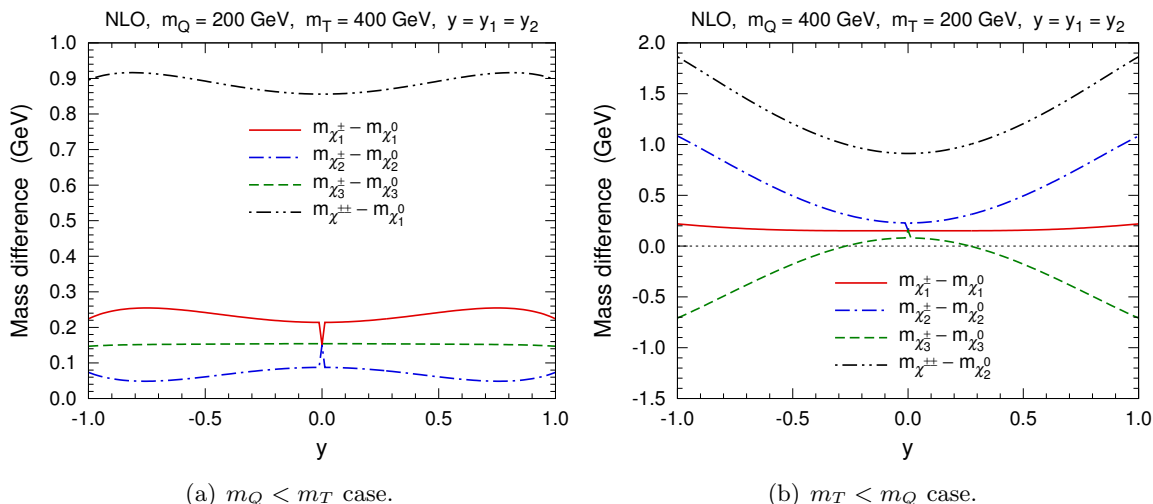


**Figure 2.** NLO mass differences between charged and neutral fermions in the custodial symmetry limit  $y = y_1 = y_2$ . The left (right) panel corresponds to  $m_Q = 200$  (400) GeV and  $m_T = 400$  (200) GeV.

Explicit expressions for the self-energies of dark sector fermions at NLO can be found in appendix B. We evaluate the mass corrections numerically with LoopTools [25]. In the custodial symmetry limit  $y = y_1 = y_2$ , the mass differences between charged and neutral fermions at NLO are presented in figure 2.  $m_{\chi_1^\pm} - m_{\chi_1^0}$ ,  $m_{\chi_2^\pm} - m_{\chi_2^0}$ , and  $m_{\chi_3^\pm} - m_{\chi_3^0}$  are degenerate for  $y = 0$ , where the triplet has no mixing with the quadruplets, and the mass splitting is solely induced by the irreducible  $\mathcal{O}(100)$  MeV contribution from the electroweak gauge interaction at one loop [10]. This degeneracy lifts for  $y \neq 0$ . When  $m_Q = 200$  GeV and  $m_T = 400$  GeV, the charged fermions are always heavier than their corresponding neutral fermions for  $|y| \leq 1$ . When  $m_Q = 400$  GeV and  $m_T = 200$  GeV,  $\chi_3^\pm$  becomes lighter than  $\chi_3^0$  for  $0.25 \lesssim |y| \leq 1$ . In both cases,  $\chi_1^0$  is always the lightest dark sector fermion as required for a DM candidate.

Moving beyond the custodial symmetry limit, in figure 3, we fix  $m_Q$ ,  $m_T$ , and  $y_1 = 1$ , and plot the fermion masses as functions of  $y_2$ . We find that a value of  $y_2$  unequal to  $y_1$  tends to drive  $\chi_1^0$  lighter, especially when the sign of  $y_2$  is opposite to  $y_1$ . The charged fermions remain rather degenerate with the corresponding neutral fermions. In figure 4, we present the corresponding mass differences, which change sign frequently as  $y_2$  varies. For  $-1.95 \lesssim y_2 \lesssim -0.5$  ( $-1.95 \lesssim y_2 \lesssim -0.85$ ) in the  $m_Q < m_T$  ( $m_T < m_Q$ ) case,  $\chi_1^0$  becomes lighter than  $\chi_1^\pm$  and fails to describe viable DM.

## 5 Constraints and relic density

In this section, we investigate the constraints on the parameter space from electroweak precision measurements, direct and indirect searches, and identify regions where the observed DM relic abundance is obtained for a standard cosmology. We discuss each of these regions in greater detail below, but begin with a summary presented in figure 5 in the  $m_Q$ - $m_T$  plane

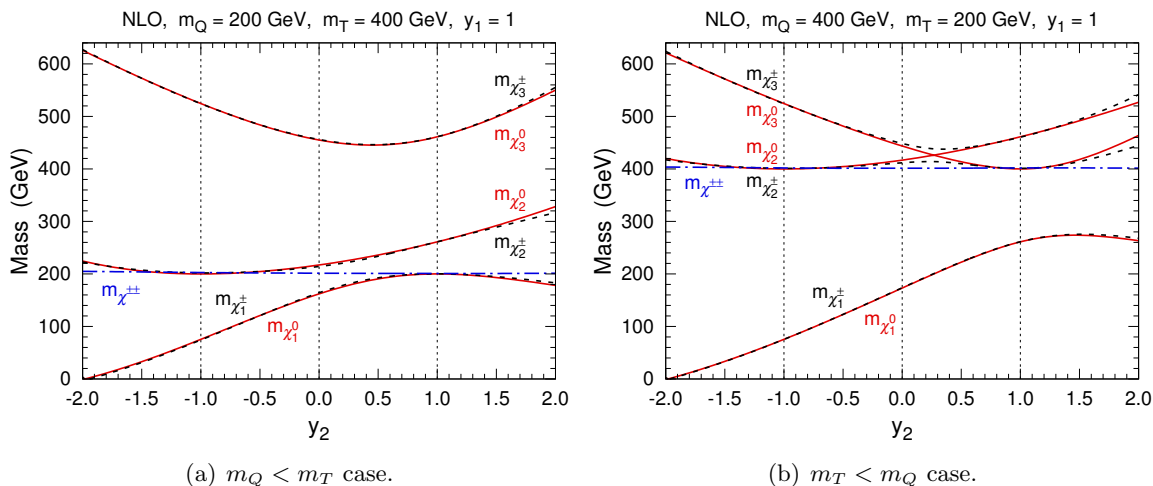


**Figure 3.** NLO fermion masses as functions of  $y_2$  for  $y_1 = 1$ . In the left (right) panel,  $m_Q = 200$  (400) GeV and  $m_T = 400$  (200) GeV. The red solid lines correspond to the neutral fermions, while the black dashed and blue dot-dashed lines correspond to the singly and doubly charged fermions, respectively.

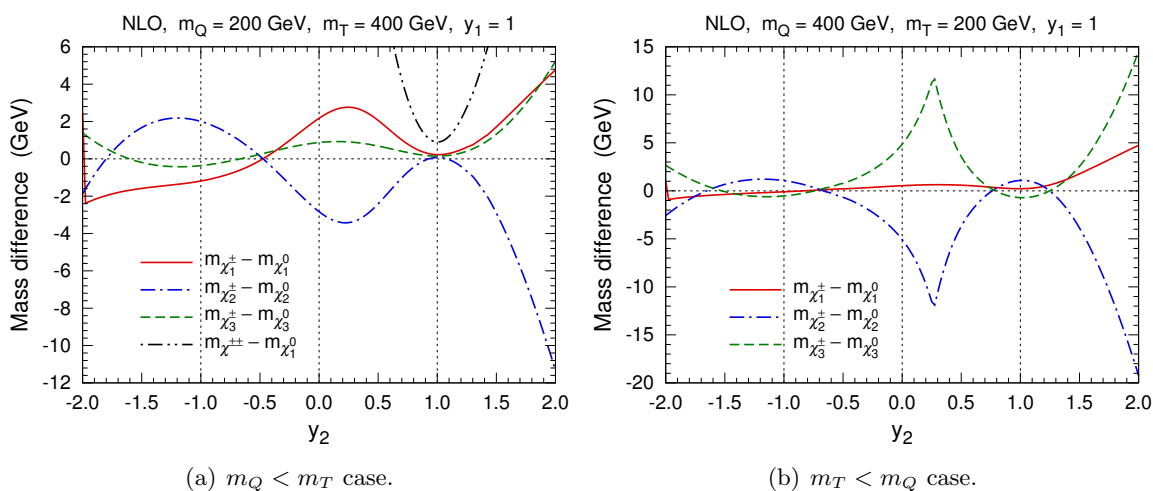


**Figure 4.** Mass differences at NLO between charged and neutral fermions as functions of  $y_2$  for  $y_1 = 1$ . In the left (right) panel,  $m_Q = 200$  (400) GeV and  $m_T = 400$  (200) GeV.

with the values of  $y_1$  and  $y_2$  fixed for four cases: (a)  $y_1 = y_2 = 0.5$  (custodial symmetry limit); (b)  $y_1 = 0.5$  and  $y_2 = 1$ ; (c)  $y_1 = 0.5$  and  $y_2 = -0.5$ ; (d)  $y_1 = 0.5$  and  $y_2 = -1$ . The dashed lines in the plots denote the contours for  $m_{\chi_1^0} = 1, 2, \text{ and } 3$  TeV. When  $y_1 v$  and  $y_2 v$  are much smaller than  $m_Q$  and  $m_T$ ,  $\chi_1^0$  is mainly constituted from the lighter multiplet. Thus we find that  $m_{\chi_1^0} \simeq m_Q$  for  $m_Q < m_T$  and  $m_{\chi_1^0} \simeq m_T$  for  $m_T < m_Q$  in figure 5. As we have seen in figure 4, when  $y_2$  has a sign opposite to  $y_1$ ,  $\chi_1^\pm$  may be lighter than  $\chi_1^0$ . Therefore, in the cases (c) and (d) the condition  $m_{\chi_1^\pm} < m_{\chi_1^0}$  (which implies that  $\chi_1^0$  is not stable) excludes large portions of the parameter space, particularly when  $m_Q < m_T$ , as shown by the violet regions in figures 5(c) and 5(d).

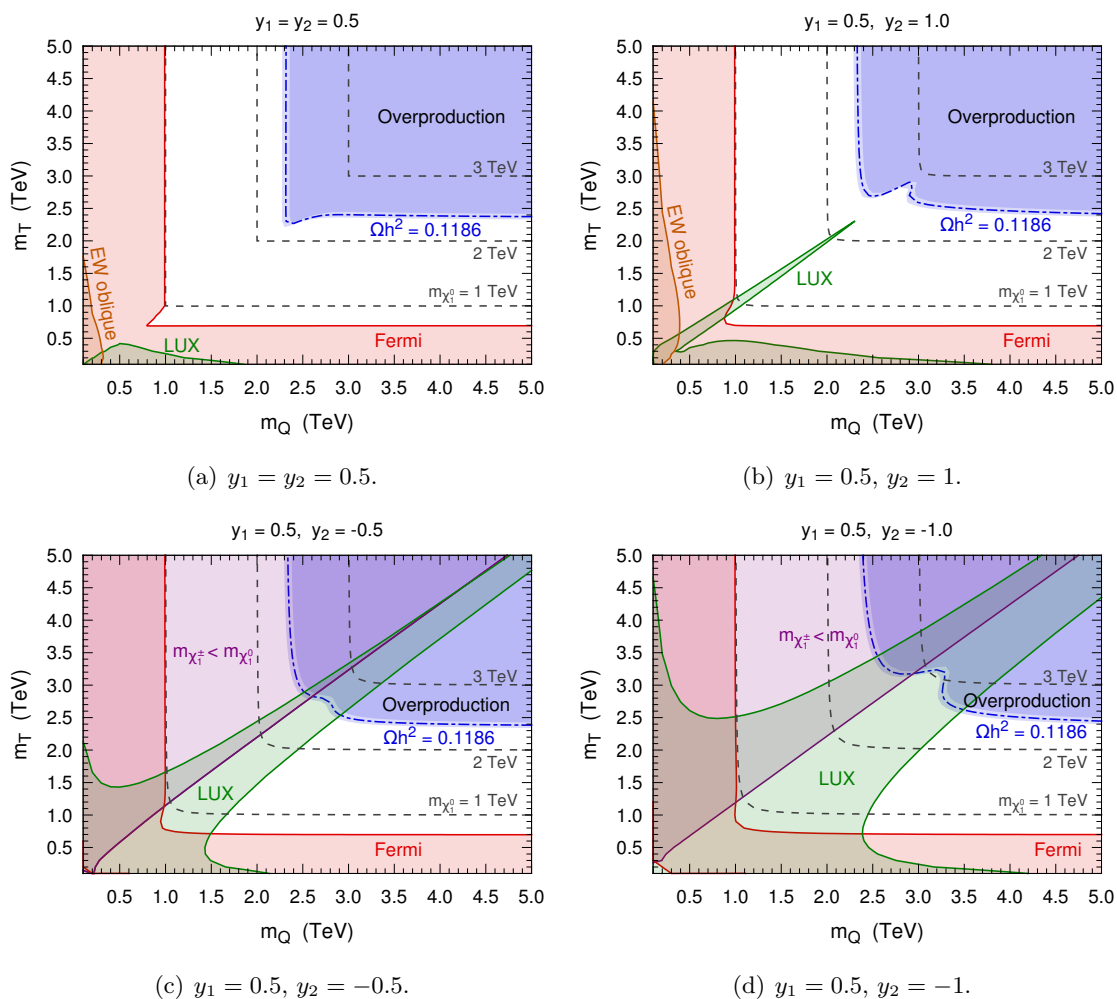


**Figure 5.** Constraints in the  $m_Q$ - $m_T$  plane for four sets of fixed  $y_1$  and  $y_2$ . The dot-dashed lines correspond to the mean value of the observed DM relic abundance [26], while the light blue bands denote its  $2\sigma$  range and the dark blue regions indicate DM overproduction in the early Universe. The violet, orange, green, and red regions are excluded by the condition  $m_{\chi_1^\pm} < m_{\chi_1^0}$ , electroweak oblique parameters [27], the LUX direct detection experiment [28], and the Fermi-LAT gamma-ray observations on dwarf galaxies [29], respectively. The gray dashed lines indicate contours of fixed  $m_{\chi_1^0}$ .

## 5.1 Relic abundance

To begin with, we identify the regions in which the dark matter abundance saturates observations for a standard cosmology. As we have seen,  $\chi_1^0$  is always nearly degenerate in mass with  $\chi_1^\pm$ . Furthermore, for  $m_Q < m_T$ , we may have  $m_{\chi^\pm} \simeq m_{\chi_1^0}$ , as well as  $m_{\chi_2^0} \simeq m_{\chi_2^\pm} \simeq m_{\chi_1^0}$  when  $m_Q \gg |y_{1,2}v|$ . These fermions, with close masses and comparable interaction strengths, tend to decouple at the same time, with coannihilation processes playing a significant role in their final abundances. Since after freeze-out they decay into  $\chi_1^0$ , we compute their combined relic abundance using the technology of ref. [30]. We implement the triplet-quadruplet model in Feynrules 2 [31], and compute the relic density with MadDM [32] (based on MadGraph 5 [33]).

In figure 5, the parameter space consistent with the DM abundance measured by the Planck experiment,  $\Omega h^2 = 0.1186 \pm 0.020$  [26], is plotted as the dot-dashed blue lines, with the  $2\sigma$  region around it denoted by the light blue shading. As is typical for an electroweakly-interacting WIMP, the observed DM abundance is realized for  $m_{\chi_1^0} \sim 2.4$  TeV. When  $\chi_1^0$  is heavier, there is effectively overproduction of DM in the early Universe, as shown by darker blue shaded regions in figure 5. Regions with lighter masses and underproduction of dark matter are left unshaded.

## 5.2 Precision electroweak constraints

The dark fermions contribute at the one loop level to precision electroweak processes. Since there are no direct coupling to the SM fermions, these take the form of corrections to the electroweak boson propagators, and are encapsulated in the oblique parameters  $S$ ,  $T$ , and  $U$  [34, 35],

$$S \equiv \frac{16\pi c_W^2 s_W^2}{e^2} \left[ \Pi'_{ZZ}(0) - \frac{c_W^2 - s_W^2}{c_W s_W} \Pi'_{ZA}(0) - \Pi'_{AA}(0) \right], \quad (5.1)$$

$$T \equiv \frac{4\pi}{e^2} \left[ \frac{\Pi_{WW}(0)}{m_W^2} - \frac{\Pi_{ZZ}(0)}{m_Z^2} \right], \quad (5.2)$$

$$U \equiv \frac{16\pi s_W^2}{e^2} \left[ \Pi'_{WW}(0) - c_W^2 \Pi'_{ZZ}(0) - 2c_W s_W \Pi'_{ZA}(0) - s_W^2 \Pi'_{AA}(0) \right], \quad (5.3)$$

where  $s_W \equiv \sin \theta_W$ ,  $c_W \equiv \cos \theta_W$  with  $\theta_W$  denoting the Weinberg angle.  $\Pi_{IJ}(p^2)$  is the  $g_{\mu\nu}$  coefficient for the vacuum polarization amplitude of gauge bosons  $I$  and  $J$ , which can be divided as  $i\Pi'_{IJ}(p^2) = ig^{\mu\nu}\Pi_{IJ}(p^2) + (p^\mu p^\nu \text{ terms})$ , and  $\Pi'_{IJ}(0) \equiv \partial\Pi_{IJ}(p^2)/\partial(p^2)|_{p^2=0}$ .

The contributions to  $\Pi_{ZZ}(p^2)$ ,  $\Pi_{WW}(p^2)$ ,  $\Pi_{AA}(p^2)$ , and  $\Pi_{ZA}(p^2)$  from dark sector fermions are given in appendix B. In the custodial symmetry limit,  $T$  and  $U$  remain zero, while  $S$  is positive and increases as  $|y|$  increases. Outside of the custodial limit, all are typically nonzero, with  $U$  typically much smaller than  $S$  and  $T$ , as is expected given the fact that it corresponds to a higher dimensional operator.

A global fit to current measurements of precision data by the Gfitter Group yields [27]

$$S = 0.05 \pm 0.11, \quad T = 0.09 \pm 0.13, \quad U = 0.01 \pm 0.11, \quad (5.4)$$

with correlation coefficients,

$$\rho_{ST} = +0.90, \quad \rho_{SU} = -0.59, \quad \rho_{TU} = -0.83. \quad (5.5)$$

These results exclude the orange regions in figures 5(a) and 5(b) at the 95% CL. In the custodial symmetry limit  $y_1 = y_2 = 0.5$ , a region limited by  $m_Q \lesssim 300$  GeV and  $m_T \lesssim 1.8$  TeV is excluded. For  $y_1 = 0.5$  and  $y_2 = 1$ , a region limited by  $m_Q \lesssim 400$  GeV and  $m_T \lesssim 4.1$  TeV is excluded.

## 5.3 Scattering with heavy nuclei

Spin-independent scattering with heavy nuclei is mediated at tree level by the exchange of a Higgs or  $Z$  boson. The coupling strength of  $\chi_1^0$  to Higgs (see appendix A) is:

$$g_{hX_1^0 X_1^0} = \frac{1}{2}(a_h X_1^0 X_1^0 + b_h X_1^0 X_1^0) = -\frac{2}{\sqrt{3}}(y_1 \mathcal{N}_{21} - y_2 \mathcal{N}_{31}) \mathcal{N}_{11}. \quad (5.6)$$

In the zero momentum transfer limit, this induces a scalar interaction with nucleons  $N$ :

$$\mathcal{L}_{S,N} = \sum_{N=p,n} G_{S,N} \bar{X}_1^0 X_1^0 \bar{N} N, \quad (5.7)$$

where

$$G_{S,N} = -\frac{g_h X_1^0 X_1^0 m_N}{2v m_h^2} \left( \sum_{q=u,d,s} f_q^N + 3f_Q^N \right), \quad (5.8)$$

and the nucleon form factors  $f_i^N$  are determined to be roughly [36]:

$$\begin{aligned} f_u^p &= 0.020 \pm 0.004, & f_d^p &= 0.026 \pm 0.005, & f_u^n &= 0.014 \pm 0.003, \\ f_d^n &= 0.036 \pm 0.008, & f_s^p &= f_s^n = 0.118 \pm 0.062, & f_Q^N &= \frac{2}{27} \left( 1 - \sum_{q=u,d,s} f_q^N \right). \end{aligned} \quad (5.9)$$

The tiny up and down Yukawa couplings imply approximately iso-symmetric couplings,  $G_{S,n} \simeq G_{S,p}$ , yielding a spin-independent (SI) scattering cross section of

$$\sigma_{\chi N}^{\text{SI}} = \frac{4}{\pi} \mu_{\chi N}^2 G_{S,N}^2, \quad (5.10)$$

where  $\mu_{\chi N} \equiv m_{\chi_1^0} m_N / (m_{\chi_1^0} + m_N)$  is the  $\chi_1^0$ - $N$  reduced mass.

As a Majorana fermion,  $\chi_1^0$  couples to  $Z$  with an axial vector coupling of strength

$$g_{Z\chi_1^0\chi_1^0} = \frac{1}{2} (b_{Z\chi_1^0\chi_1^0} - a_{Z\chi_1^0\chi_1^0}) = \frac{g}{2c_W} (|\mathcal{N}_{31}|^2 - |\mathcal{N}_{21}|^2), \quad (5.11)$$

leading to axial vector interactions with nucleons:

$$\mathcal{L}_{A,N} = \sum_{N=p,n} G_{A,N} \bar{X}_1^0 \gamma^\mu \gamma_5 X_1^0 \bar{N} \gamma^\mu \gamma_5 N, \quad (5.12)$$

where

$$G_{A,q} = \frac{g g_A^q g_{Z\chi_1^0\chi_1^0}}{4c_W m_Z^2} \text{ and } G_{A,N} = \sum_{q=u,d,s} G_{A,q} \Delta_q^N \text{ with } g_A^u = \frac{1}{2} \text{ and } g_A^d = g_A^s = -\frac{1}{2}. \quad (5.13)$$

The form factors are  $\Delta_u^p = \Delta_d^n = 0.842 \pm 0.012$ ,  $\Delta_d^p = \Delta_u^n = -0.427 \pm 0.013$ ,  $\Delta_s^p = \Delta_s^n = -0.085 \pm 0.018$  [37]. These interactions lead to a spin-dependent (SD) scattering cross section

$$\sigma_{\chi N}^{\text{SD}} = \frac{12}{\pi} \mu_{\chi N}^2 G_{A,N}^2. \quad (5.14)$$

Current limits on  $\sigma_{\chi N}^{\text{SI}}$  are lower than those on  $\sigma_{\chi N}^{\text{SD}}$  by several orders of magnitude (owing to the coherent enhancement of the SI rate for heavy nuclear targets such as Xenon). The green regions in figure 5 are excluded by the 90% CL exclusion limit on the SI DM-nucleon scattering cross section from LUX [28]. The profiles of these regions depend on the relation between  $y_1$  and  $y_2$ . As mentioned in section 3, in the custodial symmetry limit  $g_h X_1^0 X_1^0$  and  $g_{Z\chi_1^0\chi_1^0}$  vanish for  $m_Q < m_T$ , while  $g_h X_1^0 X_1^0$  is nonzero for  $m_T < m_Q$ , explaining why LUX only excludes the region with  $m_T < m_Q$  in figure 5(a) for  $y_1 = y_2 = 0.5$ . In figures 5(c) and 5(d), the exclusion regions lying around the diagonals of the plots can reach as high as  $m_{\chi_1^0} \gtrsim 5$  TeV, because  $g_h X_1^0 X_1^0$  is enhanced when  $m_Q \simeq m_T$  leads to comparable triplet and quadruplet components of  $\chi_1^0$ .

## 5.4 Dark matter annihilation

Finally, we consider bounds on the annihilation cross section  $\langle\sigma_{\text{ann}}v_{\text{rel}}\rangle$  (where  $v_{\text{rel}}$  is the relative velocity between two incoming DM particles) based on the non-observation of anomalous sources of high energy gamma rays. We adapt `MadGraph 5` to calculate the annihilation cross sections in the non-relativistic limit for all open two-body SM final states. The dominant channels<sup>2</sup> are  $W^+W^-$ ,  $ZZ$ , and  $Zh$ . The  $W^+W^-$  channel is typically dominant over  $ZZ$  and  $Zh$  by one to two orders of magnitude.

Thus, we compare predictions for annihilation into  $W^+W^-$  with the null results for evidence of DM annihilation into gamma rays in dwarf spheroidal galaxies based on 6 years of data collected by the *Fermi*-LAT experiment [29]. *Fermi* provides 95% CL upper limits on  $\langle\sigma_{\text{ann}}v_{\text{rel}}\rangle$  for annihilation into  $W^+W^-$  as a function of the DM particle mass, which we translate into the exclusion regions shown as the red shaded regions in figure 5. The *Fermi* data basically excludes  $m_{\chi_1^0} \lesssim 1$  TeV for  $m_Q < m_T$  and  $m_{\chi_1^0} \lesssim 700$  GeV for  $m_T < m_Q$ .

## 5.5 Constraints on the $y_1$ - $y_2$ plane

By fixing the mass parameters  $m_T$  and  $m_Q$ , we can see how the constraints vary in the  $y_1$ - $y_2$  plane, as shown in figure 6. The plots are symmetric under the simultaneous transformations of  $y_1 \rightarrow -y_1$  and  $y_2 \rightarrow -y_2$ . In figures 6(a) and 6(c), we have  $m_Q < m_T$ , and the condition  $m_{\chi_1^\pm} < m_{\chi_1^0}$  excludes some regions where  $y_1$  and  $y_2$  are sufficiently large and their signs are opposite to each other. The contours of  $m_{\chi_1^0}$  are parallel to the diagonals, which correspond to the custodial symmetry limit and have the largest values of  $m_{\chi_1^0}$ . In figures 6(b) and 6(d), we have  $m_T < m_Q$ , and  $m_{\chi_1^0}$  is larger at the corners of  $y_1 = y_2 = 1.5$  and  $y_1 = y_2 = -1.5$  than at the corners of  $y_1 = -y_2 = 1.5$  and  $y_1 = -y_2 = -1.5$ .

In figures 6(a) and 6(b), the fixed values of  $m_T$  and  $m_Q$  are suitable for obtaining an observed DM abundance. The contours corresponding to the mean value of the measured  $\Omega h^2$  appear as ellipses, inside which  $\Omega h^2$  is larger. The mass parameters are chosen to show comparable sensitivities of LUX and *Fermi*-LAT in figures 6(c) and 6(d), where both the LUX and *Fermi* exclusion regions enclose the point  $y_1 = -y_2 = 1.5$  as well as the point  $y_1 = -y_2 = -1.5$ . In figure 6(d), the LUX bound also excludes the regions around  $y_1 = y_2 = 1.5$  and  $y_1 = y_2 = -1.5$ . Both the LUX and *Fermi* limits roughly coincide with the contours of  $m_{\chi_1^0}$ .

## 6 Conclusions and outlook

In this work, we explore a dark sector consisting of a fermionic  $SU(2)_L$  triplet and two fermionic  $SU(2)_L$  quadruplets. This set-up is a minimal UV complete realistic model of electroweakly interacting dark matter with tree level coupling to the SM Higgs boson, the simplest such construction which is distinct from any limit of the MSSM. After electroweak symmetry-breaking, the dark sector consists of three Majorana fermions  $\chi_i^0$ , three singly charged fermions  $\chi_i^\pm$ , and one doubly charged fermion  $\chi^{\pm\pm}$ . The lightest neutral fermion  $\chi_1^0$  is a wonderful DM candidate provided it is the lightest of the dark sector fermions.

<sup>2</sup>Annihilation into fermions mediated by the  $Z$  or  $h$  bosons and into  $hh$  are suppressed by either  $v_{\text{rel}}^2$ ,  $m_f^2/m_{\chi_1^0}^2$ , both [38].

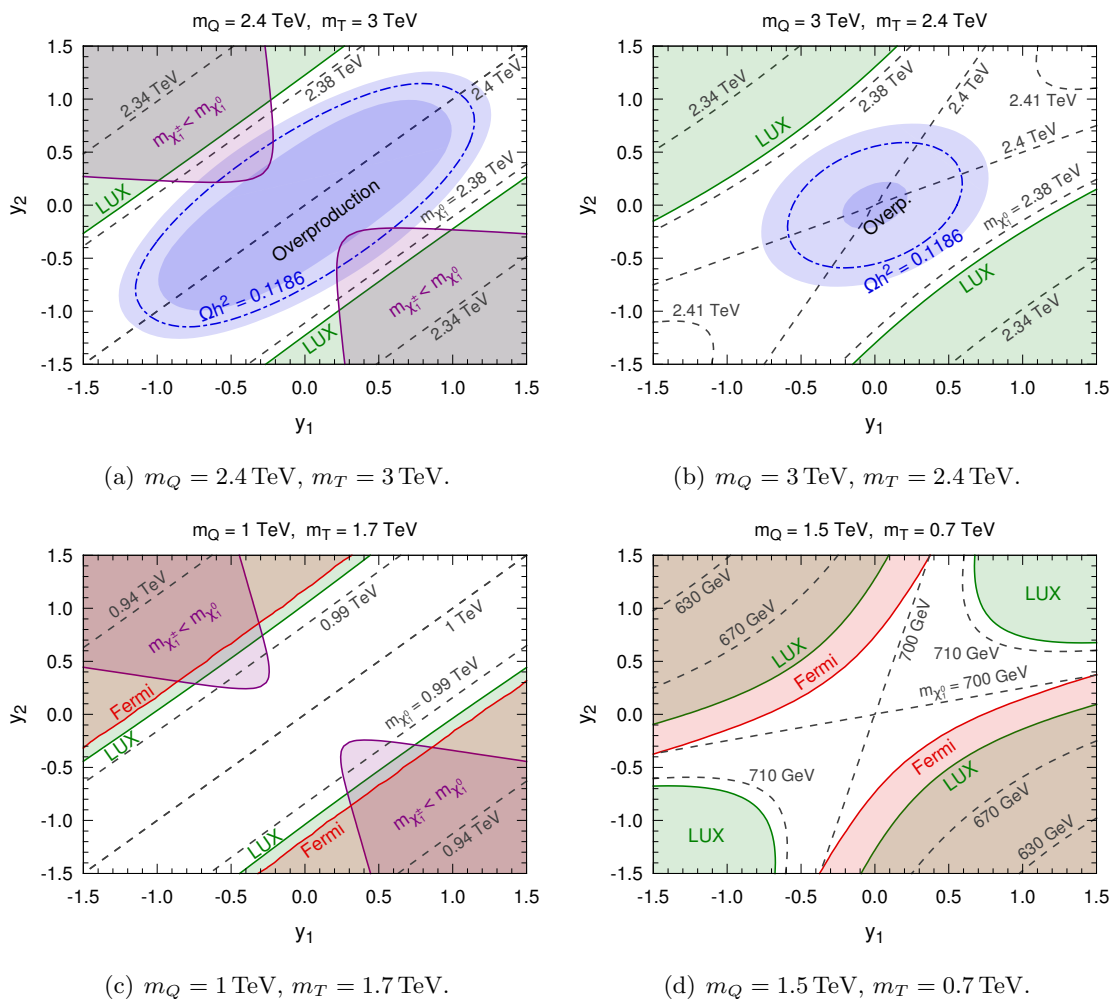


**Figure 6.** Constraints on the  $y_1$ - $y_2$  plane for four sets of fixed  $m_Q$  and  $m_T$  as indicated. The legend for the lines and shadings are the same as in figure 5.

When two Yukawa couplings are equal, i.e.,  $y_1 = y_2$ , there is an approximate global custodial symmetry, implying that  $\chi_i^0$  is mass-degenerate with  $\chi_i^\pm$  at tree level. We compute the one-loop mass corrections to determine the precise spectrum. Fortunately, in the custodial limit these corrections always increase the masses of charged fermions. Another gift from this symmetry is the tree-level vanishing of the  $\chi_1^0$  couplings to  $Z$  and  $h$ , rendering the current DM direct searches impotent as far as constraining it. Beyond the custodial symmetry limit, at tree level  $m_{\chi_i^0}$  and  $m_{\chi_i^\pm}$  are slightly different, but nonetheless still quite degenerate. At the one-loop level, mass corrections suggest that we may have  $m_{\chi_1^\pm} < m_{\chi_1^0}$  when  $y_1$  and  $y_2$  have opposite signs. When that happens,  $\chi_1^0$  is no longer a viable DM candidate, decaying into the lightest charged state.

Due to the mass degeneracy, coannihilation processes among dark sector fermions strongly affect the abundance evolution of  $\chi_1^0$  in the early Universe, and must be included. The calculation suggests that  $m_{\chi_1^0} \sim 2.4 \text{ TeV}$  to saturate the observed relic density for a

standard cosmology. We also investigate the constraints from the electroweak oblique parameters and direct and indirect searches. The global fit result of  $S$ ,  $T$ , and  $U$  parameters excludes a region up to  $m_Q \lesssim 300$  (400) GeV and  $m_T \lesssim 1.8$  (4.1) TeV for  $y_1 = y_2 = 0.5$  ( $y_1 = 0.5$  and  $y_2 = 1$ ). The LUX exclusion region significantly depends on the relation between  $y_1$  and  $y_2$ . When  $y_2$  has a sign opposite to  $y_1$ , the LUX result excludes  $m_{\chi_1^0}$  up to several TeV for  $m_Q \simeq m_T$ , cutting in to some regions favored by the relic abundance. Annihilation into  $W^+W^-$  is the dominant channel in the non-relativistic limit, and *Fermi*-LAT dwarf galaxy limits exclude  $m_{\chi_1^0} \lesssim 1$  TeV and  $\lesssim 700$  GeV for  $m_Q < m_T$  and  $m_T < m_Q$ , respectively. Nonetheless, there is still plenty of room in the parameter space that is consistent with the observed DM abundance and escaping from phenomenological constraints.

As the charged fermions in the dark sector couple to the Higgs boson, the  $h \rightarrow \gamma\gamma$  decay is a possible indirect probe of their presence. However, the current LHC data are not sufficiently precise to give a meaningful limit, though LHC high luminosity running may reach the correct ballpark [39]. LHC direct searches for exotic charged particles decaying into missing momentum may also be able to explore the model, but the electroweak production rates of the dark sector charged fermions are quite low for multi-TeV fermions, and it may ultimately fall to future higher energy colliders to have the last word [40, 41].

## Acknowledgments

TMPT acknowledges Randy Cotta, JoAnne Hewett, and Devin Walker for earlier collaboration on related topics. ZHY would like to acknowledge helpful discussions with Arvind Rajaraman, Philip Tanedo, Alexander Wijango, Mohammad Abdullah, and Ye-Ling Zhou and also thanks the Particle Theory Group at UC Irvine for hospitality during his visit. The work of TMPT is supported in part by NSF grant PHY-1316792 and by the University of California, Irvine through a Chancellor’s Fellowship, and that of ZHY was supported by the China Scholarship Council (Grant No. 201404910374).

## A Detailed expressions for interaction terms

In this appendix, we derive explicit expressions for the interaction terms in the triplet-quadruplet model. The covariant derivatives for the triplet and quadruplets are

$$D_\mu T = (\partial_\mu - igW_\mu^a t_T^a)T, \tag{A.1}$$

$$D_\mu Q_i = (\partial_\mu - ig'B_\mu Y_{Q_i} - igW_\mu^a t_Q^a)Q_i, \tag{A.2}$$

where  $Y_{Q_1} = -1/2$ ,  $Y_{Q_2} = +1/2$ , and the generators of  $SU(2)_L$  are:

$$t_T^1 = \frac{1}{\sqrt{2}} \begin{pmatrix} & 1 & \\ 1 & & -1 \\ & -1 & \end{pmatrix}, \quad t_T^2 = \frac{1}{\sqrt{2}} \begin{pmatrix} & -i & \\ i & & i \\ & -i & \end{pmatrix}, \quad t_T^3 = \begin{pmatrix} 1 & & \\ & 0 & \\ & & -1 \end{pmatrix}, \tag{A.3}$$

and

$$\begin{aligned}
 t_Q^1 &= \begin{pmatrix} & \sqrt{3}/2 & & \\ \sqrt{3}/2 & & 1 & \\ & 1 & & \sqrt{3}/2 \\ & & \sqrt{3}/2 & \end{pmatrix}, \quad t_Q^2 = \begin{pmatrix} & -\sqrt{3}i/2 & & \\ \sqrt{3}i/2 & & -i & \\ & i & & -\sqrt{3}i/2 \\ & & \sqrt{3}i/2 & \end{pmatrix}, \\
 t_Q^3 &= \text{diag} \left( \frac{3}{2}, \frac{1}{2}, -\frac{1}{2}, -\frac{3}{2} \right). \tag{A.4}
 \end{aligned}$$

We can express the gauge interaction terms in eqs. (2.2) and (2.3) as

$$\begin{aligned}
 \mathcal{L}_T &\supset T^\dagger \bar{\sigma}^\mu g W_\mu^a t_T^a T \\
 &= (eA_\mu + g c_W Z_\mu)(T^+)^\dagger \bar{\sigma}^\mu T^+ + g W_\mu^+ (T^+)^\dagger \bar{\sigma}^\mu T^0 + g W_\mu^- (T^0)^\dagger \bar{\sigma}^\mu T^+ \\
 &\quad - g W_\mu^+ (T^0)^\dagger \bar{\sigma}^\mu T^- - g W_\mu^- (T^-)^\dagger \bar{\sigma}^\mu T^0 - (eA_\mu + g c_W Z_\mu)(T^-)^\dagger \bar{\sigma}^\mu T^- \tag{A.5}
 \end{aligned}$$

and

$$\begin{aligned}
 \mathcal{L}_Q &\supset Q_1^\dagger \bar{\sigma}^\mu (g' B_\mu Y_{Q_1} + g W_\mu^a t_Q^a) Q_1 + Q_2^\dagger \bar{\sigma}^\mu (g' B_\mu Y_{Q_2} + g W_\mu^a t_Q^a) Q_2 \\
 &= \frac{\sqrt{6}}{2} g W_\mu^+ [(Q_1^+)^\dagger \bar{\sigma}^\mu Q_1^0 + (Q_2^{++})^\dagger \bar{\sigma}^\mu Q_2^+] + \frac{\sqrt{6}}{2} g W_\mu^- [(Q_1^0)^\dagger \bar{\sigma}^\mu Q_1^+ + (Q_2^+)^\dagger \bar{\sigma}^\mu Q_2^{++}] \\
 &\quad + \sqrt{2} g W_\mu^+ [(Q_1^0)^\dagger \bar{\sigma}^\mu Q_1^- + (Q_2^+)^\dagger \bar{\sigma}^\mu Q_2^0] + \sqrt{2} g W_\mu^- [(Q_1^-)^\dagger \bar{\sigma}^\mu Q_1^0 + (Q_2^0)^\dagger \bar{\sigma}^\mu Q_2^+] \\
 &\quad + \frac{\sqrt{6}}{2} g W_\mu^+ [(Q_1^-)^\dagger \bar{\sigma}^\mu Q_1^{--} + (Q_2^0)^\dagger \bar{\sigma}^\mu Q_2^-] + \frac{\sqrt{6}}{2} g W_\mu^- [(Q_1^{--})^\dagger \bar{\sigma}^\mu Q_1^- + (Q_2^-)^\dagger \bar{\sigma}^\mu Q_2^0] \\
 &\quad + \frac{g}{2c_W} Z_\mu (Q_1^0)^\dagger \bar{\sigma}^\mu Q_1^0 - \frac{g}{2c_W} Z_\mu (Q_2^0)^\dagger \bar{\sigma}^\mu Q_2^0 \\
 &\quad + \left[ eA_\mu + \frac{g(s_W^2 + 3c_W^2)}{2c_W} Z_\mu \right] (Q_1^+)^\dagger \bar{\sigma}^\mu Q_1^+ + \left[ eA_\mu + \frac{g(c_W^2 - s_W^2)}{2c_W} Z_\mu \right] (Q_2^+)^\dagger \bar{\sigma}^\mu Q_2^+ \\
 &\quad + \left[ -eA_\mu + \frac{g(s_W^2 - c_W^2)}{2c_W} Z_\mu \right] (Q_1^-)^\dagger \bar{\sigma}^\mu Q_1^- + \left[ -eA_\mu - \frac{g(3c_W^2 + s_W^2)}{2c_W} Z_\mu \right] (Q_2^-)^\dagger \bar{\sigma}^\mu Q_2^- \\
 &\quad + \left[ -2eA_\mu + \frac{g(s_W^2 - 3c_W^2)}{2c_W} Z_\mu \right] (Q_1^{--})^\dagger \bar{\sigma}^\mu Q_1^{--} \\
 &\quad + \left[ 2eA_\mu + \frac{g(3c_W^2 - s_W^2)}{2c_W} Z_\mu \right] (Q_2^{++})^\dagger \bar{\sigma}^\mu Q_2^{++}. \tag{A.6}
 \end{aligned}$$

Including the would-be Goldstone bosons, eq. (2.4) becomes

$$\begin{aligned}
 \mathcal{L}_{\text{HTQ}} &= y_1 G^+ \left( Q_1^{--} T^+ - \frac{2}{\sqrt{6}} Q_1^- T^0 - \frac{1}{\sqrt{3}} Q_1^0 T^- \right) \\
 &\quad + y_1 (v + h + iG^0) \left( \frac{1}{\sqrt{6}} Q_1^- T^+ - \frac{1}{\sqrt{3}} Q_1^0 T^0 - \frac{1}{\sqrt{2}} Q_1^+ T^- \right) \\
 &\quad + y_2 G^- \left( -Q_2^{++} T^- - \frac{2}{\sqrt{6}} Q_2^+ T^0 + \frac{1}{\sqrt{3}} Q_2^0 T^+ \right) \\
 &\quad + y_2 (v + h - iG^0) \left( \frac{1}{\sqrt{3}} Q_2^0 T^0 + \frac{1}{\sqrt{6}} Q_2^+ T^- - \frac{1}{\sqrt{2}} Q_2^- T^+ \right) + \text{h.c.}, \tag{A.7}
 \end{aligned}$$

where the Goldstone bosons  $G^0$  and  $G^\pm$  are defined as

$$H = \begin{pmatrix} H^+ \\ H^0 \end{pmatrix} = \begin{pmatrix} G^+ \\ \frac{1}{\sqrt{2}}(v + h + iG^0) \end{pmatrix}. \quad (\text{A.8})$$

For convenience, we would like to express the interaction terms with 4-component fermionic fields. Here we define

$$\Psi_i^0 = \begin{pmatrix} \psi_{iL}^0 \\ (\psi_{iR}^0)^\dagger \end{pmatrix}, \quad \Psi_i^+ = \begin{pmatrix} \psi_{iL}^+ \\ (\psi_{iR}^-)^\dagger \end{pmatrix}, \quad (\text{A.9})$$

where

$$\psi_L^0 = \psi_R^0 = (T^0, Q_1^0, Q_2^0)^T, \quad \psi_L^+ = (T^+, Q_1^+, Q_2^+)^T, \quad \psi_R^- = (T^-, Q_1^-, Q_2^-)^T. \quad (\text{A.10})$$

Now eq. (2.22) is equivalent to

$$\psi_{L,R}^0 = \mathcal{N}\chi_{L,R}^0, \quad \psi_L^+ = \mathcal{C}_L\chi_L^+, \quad \psi_R^- = \mathcal{C}_R\chi_R^-. \quad (\text{A.11})$$

We can use chiral projection operators to divide every fermionic field into two parts:

$$\Psi_{iL}^{0,+} = P_L\Psi_i^{0,+}, \quad \Psi_{iR}^{0,+} = P_R\Psi_i^{0,+}, \quad X_{iL}^{0,+,++} = P_LX_i^{0,+,++}, \quad X_{iR}^{0,+,++} = P_RX_i^{0,+,++}. \quad (\text{A.12})$$

Thus we have

$$\Psi_{iL}^0 = \mathcal{N}_{ij}X_{jL}^0, \quad \Psi_{iR}^0 = \mathcal{N}_{ij}^*X_{jR}^0, \quad \Psi_{iL}^+ = (\mathcal{C}_L)_{ij}X_{jL}^+, \quad \Psi_{iR}^+ = (\mathcal{C}_R)_{ij}^*X_{jR}^+. \quad (\text{A.13})$$

The interaction terms in eqs. (A.5), (A.6), and (A.7) can be written down with the 4-component fields  $\Psi_i^0$  and  $\Psi_i^+$  projected into their left- and right-handed parts:

$$\begin{aligned} \mathcal{L}_\Psi = & a_{A\Psi_i^+\Psi_j^+}A_\mu\bar{\Psi}_{iL}^+\gamma^\mu\Psi_{jL}^+ + b_{A\Psi_i^+\Psi_j^+}A_\mu\bar{\Psi}_{iR}^+\gamma^\mu\Psi_{jR}^+ + a_{Z\Psi_i^+\Psi_j^+}Z_\mu\bar{\Psi}_{iL}^+\gamma^\mu\Psi_{jL}^+ \\ & + b_{Z\Psi_i^+\Psi_j^+}Z_\mu\bar{\Psi}_{iR}^+\gamma^\mu\Psi_{jR}^+ + \frac{1}{2}(a_{Z\Psi_i^0\Psi_j^0}Z_\mu\bar{\Psi}_{iL}^0\gamma^\mu\Psi_{jL}^0 + b_{Z\Psi_i^0\Psi_j^0}Z_\mu\bar{\Psi}_{iR}^0\gamma^\mu\Psi_{jR}^0) \\ & + a_{W\Psi_i^+\Psi_j^0}(W_\mu^+\bar{\Psi}_{iL}^+\gamma^\mu\Psi_{jL}^0 + \text{h.c.}) + b_{W\Psi_i^+\Psi_j^0}(W_\mu^+\bar{\Psi}_{iR}^+\gamma^\mu\Psi_{jR}^0 + \text{h.c.}) \\ & + a_{WX^{++}\Psi_i^+}(W_\mu^+\bar{X}_{iL}^{++}\gamma^\mu\Psi_{iL}^+ + \text{h.c.}) + b_{WX^{++}\Psi_i^+}(W_\mu^+\bar{X}_{iR}^{++}\gamma^\mu\Psi_{iR}^+ + \text{h.c.}) \\ & + \frac{1}{2}(a_{h\Psi_i^0\Psi_j^0}h\bar{\Psi}_{iR}^0\Psi_{jL}^0 + b_{h\Psi_i^0\Psi_j^0}h\bar{\Psi}_{iL}^0\Psi_{jR}^0 + a_{G^0\Psi_i^0\Psi_j^0}G^0\bar{\Psi}_{iR}^0\Psi_{jL}^0 + b_{G^0\Psi_i^0\Psi_j^0}G^0\bar{\Psi}_{iL}^0\Psi_{jR}^0) \\ & + a_{h\Psi_i^+\Psi_j^+}h\bar{\Psi}_{iR}^+\Psi_{jL}^+ + b_{h\Psi_i^+\Psi_j^+}h\bar{\Psi}_{iL}^+\Psi_{jR}^+ + a_{G^0\Psi_i^+\Psi_j^+}G^0\bar{\Psi}_{iR}^+\Psi_{jL}^+ + b_{G^0\Psi_i^+\Psi_j^+}G^0\bar{\Psi}_{iL}^+\Psi_{jR}^+ \\ & + a_{G^\pm\Psi_i^+\Psi_j^0}(G^+\bar{\Psi}_{iR}^+\Psi_{jL}^0 + \text{h.c.}) + b_{G^\pm\Psi_i^+\Psi_j^0}(G^+\bar{\Psi}_{iL}^+\Psi_{jR}^0 + \text{h.c.}) \\ & + a_{G^\pm X^{++}\Psi_i^+}(G^+\bar{X}_{iR}^{++}\Psi_{iL}^+ + \text{h.c.}) + b_{G^\pm X^{++}\Psi_i^+}(G^+\bar{X}_{iL}^{++}\Psi_{iR}^+ + \text{h.c.}), \end{aligned} \quad (\text{A.14})$$

where the coupling coefficients read

$$\begin{aligned} a_{A\Psi_1^+\Psi_1^+} &= b_{A\Psi_1^+\Psi_1^+} = a_{A\Psi_2^+\Psi_2^+} = b_{A\Psi_2^+\Psi_2^+} = a_{A\Psi_3^+\Psi_3^+} = b_{A\Psi_3^+\Psi_3^+} = e, \\ a_{Z\Psi_1^+\Psi_1^+} &= b_{Z\Psi_1^+\Psi_1^+} = gc_W, \quad a_{Z\Psi_2^+\Psi_2^+} = \frac{g}{2c_W}(3c_W^2 + s_W^2) = b_{Z\Psi_3^+\Psi_3^+}, \end{aligned}$$

$$\begin{aligned}
 b_{Z\Psi_2^+\Psi_2^+} &= \frac{g}{2c_W}(c_W^2 - s_W^2) = a_{Z\Psi_3^+\Psi_3^+}, \\
 a_{Z\Psi_2^0\Psi_2^0} &= -b_{Z\Psi_2^0\Psi_2^0} = \frac{g}{2c_W}, \quad a_{Z\Psi_3^0\Psi_3^0} = -b_{Z\Psi_3^0\Psi_3^0} = -\frac{g}{2c_W}, \\
 a_{W\Psi_1^+\Psi_1^0} &= b_{W\Psi_1^+\Psi_1^0} = g, \quad a_{W\Psi_2^+\Psi_2^0} = \frac{\sqrt{6}}{2}g = -b_{W\Psi_3^+\Psi_3^0}, \quad b_{W\Psi_2^+\Psi_2^0} = -\sqrt{2}g = -a_{W\Psi_3^+\Psi_3^0}, \\
 b_{WX^{++}\Psi_2^+} &= -\frac{\sqrt{6}}{2}g, \quad a_{WX^{++}\Psi_3^+} = \frac{\sqrt{6}}{2}g, \\
 a_{h\Psi_1^0\Psi_2^0} &= b_{h\Psi_1^0\Psi_2^0} = -\frac{y_1}{\sqrt{3}} = a_{h\Psi_2^0\Psi_1^0} = b_{h\Psi_2^0\Psi_1^0}, \\
 a_{h\Psi_1^0\Psi_3^0} &= b_{h\Psi_1^0\Psi_3^0} = \frac{y_2}{\sqrt{3}} = a_{h\Psi_3^0\Psi_1^0} = b_{h\Psi_3^0\Psi_1^0}, \\
 a_{G^0\Psi_1^0\Psi_2^0} &= -b_{G^0\Psi_1^0\Psi_2^0} = -\frac{y_1}{\sqrt{3}}i = a_{G^0\Psi_2^0\Psi_1^0} = -b_{G^0\Psi_2^0\Psi_1^0}, \\
 a_{G^0\Psi_1^0\Psi_3^0} &= -b_{G^0\Psi_1^0\Psi_3^0} = -\frac{y_2}{\sqrt{3}}i = a_{G^0\Psi_3^0\Psi_1^0} = -b_{G^0\Psi_3^0\Psi_1^0}, \\
 a_{h\Psi_1^+\Psi_2^+} &= b_{h\Psi_2^+\Psi_1^+} = -\frac{y_1}{\sqrt{2}}, \quad a_{h\Psi_2^+\Psi_1^+} = b_{h\Psi_1^+\Psi_2^+} = \frac{y_1}{\sqrt{6}}, \\
 a_{h\Psi_1^+\Psi_3^+} &= b_{h\Psi_3^+\Psi_1^+} = \frac{y_2}{\sqrt{6}}, \quad a_{h\Psi_3^+\Psi_1^+} = b_{h\Psi_1^+\Psi_3^+} = -\frac{y_2}{\sqrt{2}}, \\
 a_{G^0\Psi_1^+\Psi_2^+} &= -b_{G^0\Psi_2^+\Psi_1^+} = -\frac{y_1}{\sqrt{2}}i, \quad a_{G^0\Psi_2^+\Psi_1^+} = -b_{G^0\Psi_1^+\Psi_2^+} = \frac{y_1}{\sqrt{6}}i, \\
 a_{G^0\Psi_1^+\Psi_3^+} &= -b_{G^0\Psi_3^+\Psi_1^+} = -\frac{y_2}{\sqrt{6}}i, \quad a_{G^0\Psi_3^+\Psi_1^+} = -b_{G^0\Psi_1^+\Psi_3^+} = \frac{y_2}{\sqrt{2}}i, \\
 a_{G^\pm\Psi_1^+\Psi_2^0} &= -\frac{y_1}{\sqrt{3}}, \quad a_{G^\pm\Psi_2^+\Psi_1^0} = -\frac{2y_1}{\sqrt{6}}, \quad b_{G^\pm\Psi_1^+\Psi_3^0} = \frac{y_2}{\sqrt{3}}, \quad b_{G^\pm\Psi_3^+\Psi_1^0} = -\frac{2y_2}{\sqrt{6}}, \\
 a_{G^\pm X^{++}\Psi_1^+} &= y_1, \quad b_{G^\pm X^{++}\Psi_1^+} = -y_2.
 \end{aligned} \tag{A.15}$$

The coupling coefficients that have not mentioned above are zero. Converting the gauge bases into the physical bases, we have

$$\begin{aligned}
 \mathcal{L}_X &= a_{AX_i^+X_j^+}A_\mu\bar{X}_{iL}^+\gamma^\mu X_{jL}^+ + b_{AX_i^+X_j^+}A_\mu\bar{X}_{iR}^+\gamma^\mu X_{jR}^+ + a_{ZX_i^+X_j^+}Z_\mu\bar{X}_{iL}^+\gamma^\mu X_{jL}^+ \\
 &\quad + b_{ZX_i^+X_j^+}Z_\mu\bar{X}_{iR}^+\gamma^\mu X_{jR}^+ + \frac{1}{2}(a_{ZX_i^0X_j^0}Z_\mu\bar{X}_{iL}^0\gamma^\mu X_{jL}^0 + b_{ZX_i^0X_j^0}Z_\mu\bar{X}_{iR}^0\gamma^\mu X_{jR}^0) \\
 &\quad + a_{AX^{++}X^{++}}A_\mu\bar{X}_L^{++}\gamma^\mu X_L^{++} + b_{AX^{++}X^{++}}A_\mu\bar{X}_R^{++}\gamma^\mu X_R^{++} \\
 &\quad + a_{ZX^{++}X^{++}}Z_\mu\bar{X}_L^{++}\gamma^\mu X_L^{++} + b_{ZX^{++}X^{++}}Z_\mu\bar{X}_R^{++}\gamma^\mu X_R^{++} \\
 &\quad + (a_{WX_i^+X_j^0}W_\mu^+\bar{X}_{iL}^+\gamma^\mu X_{jL}^0 + \text{h.c.}) + (b_{WX_i^+X_j^0}W_\mu^+\bar{X}_{iR}^+\gamma^\mu X_{jR}^0 + \text{h.c.}) \\
 &\quad + (a_{WX^{++}X_i^+}W_\mu^+\bar{X}_L^{++}\gamma^\mu X_{iL}^+ + \text{h.c.}) + (b_{WX^{++}X_i^+}W_\mu^+\bar{X}_R^{++}\gamma^\mu X_{iR}^+ + \text{h.c.}) \\
 &\quad + \frac{1}{2}(a_{hX_i^0X_j^0}h\bar{X}_{iR}^0X_{jL}^0 + b_{hX_i^0X_j^0}h\bar{X}_{iL}^0X_{jR}^0 + a_{G^0X_i^0X_j^0}G^0\bar{X}_{iR}^0X_{jL}^0 + b_{G^0X_i^0X_j^0}G^0\bar{X}_{iL}^0X_{jR}^0) \\
 &\quad + a_{hX_i^+X_j^+}h\bar{X}_{iR}^+X_{jL}^+ + b_{hX_i^+X_j^+}h\bar{X}_{iL}^+X_{jR}^+ + a_{G^0X_i^+X_j^+}G^0\bar{X}_{iR}^+X_{jL}^+ + b_{G^0X_i^+X_j^+}G^0\bar{X}_{iL}^+X_{jR}^+ \\
 &\quad + (a_{G^\pm X_i^+X_j^0}G^+\bar{X}_{iR}^+X_{jL}^0 + \text{h.c.}) + (b_{G^\pm X_i^+X_j^0}G^+\bar{X}_{iL}^+X_{jR}^0 + \text{h.c.}) \\
 &\quad + (a_{G^\pm X^{++}X_i^+}G^+\bar{X}_R^{++}X_{iL}^+ + \text{h.c.}) + (b_{G^\pm X^{++}X_i^+}G^+\bar{X}_L^{++}X_{iR}^+ + \text{h.c.}),
 \end{aligned} \tag{A.16}$$

where the coupling coefficients are related to those in (A.15) through the mixing matrices:

$$\begin{aligned}
 a_{AX_i^+ X_j^+} &= a_{A\Psi_k^+ \Psi_k^+} (\mathcal{C}_L)_{ki}^* (\mathcal{C}_L)_{kj} = e\delta_{ij}, & b_{AX_i^+ X_j^+} &= b_{A\Psi_k^+ \Psi_k^+} (\mathcal{C}_R)_{ki} (\mathcal{C}_R)_{kj}^* = e\delta_{ij}, \\
 a_{ZX_i^+ X_j^+} &= a_{Z\Psi_k^+ \Psi_k^+} (\mathcal{C}_L)_{ki}^* (\mathcal{C}_L)_{kj}, & b_{ZX_i^+ X_j^+} &= b_{Z\Psi_k^+ \Psi_k^+} (\mathcal{C}_R)_{ki} (\mathcal{C}_R)_{kj}^*, \\
 a_{ZX_i^0 X_j^0} &= a_{Z\Psi_k^0 \Psi_k^0} \mathcal{N}_{ki}^* \mathcal{N}_{kj}, & b_{ZX_i^0 X_j^0} &= b_{Z\Psi_k^0 \Psi_k^0} \mathcal{N}_{ki} \mathcal{N}_{kj}^*, \\
 a_{AX_{++} X_{++}} &= b_{AX_{++} X_{++}} = 2e, & a_{ZX_{++} X_{++}} &= b_{ZX_{++} X_{++}} = \frac{g}{2c_W} (3c_W^2 - s_W^2), \\
 a_{WX_i^+ X_j^0} &= a_{W\Psi_k^+ \Psi_k^0} (\mathcal{C}_L)_{ki}^* \mathcal{N}_{kj}, & b_{WX_i^+ X_j^0} &= b_{W\Psi_k^+ \Psi_k^0} (\mathcal{C}_R)_{ki} \mathcal{N}_{kj}^*, \\
 a_{WX_{++} X_i^+} &= a_{WX_{++} \Psi_j^+} (\mathcal{C}_L)_{ji}, & b_{WX_{++} X_i^+} &= b_{WX_{++} \Psi_j^+} (\mathcal{C}_R)_{ji}^*, \\
 a_{hX_i^0 X_j^0} &= a_{h\Psi_k^0 \Psi_l^0} \mathcal{N}_{ki} \mathcal{N}_{lj}, & b_{hX_i^0 X_j^0} &= b_{h\Psi_k^0 \Psi_l^0} \mathcal{N}_{ki}^* \mathcal{N}_{lj}^*, \\
 a_{G^0 X_i^0 X_j^0} &= a_{G^0 \Psi_k^0 \Psi_l^0} \mathcal{N}_{ki} \mathcal{N}_{lj}, & b_{G^0 X_i^0 X_j^0} &= b_{G^0 \Psi_k^0 \Psi_l^0} \mathcal{N}_{ki}^* \mathcal{N}_{lj}^*, \\
 a_{hX_i^+ X_j^+} &= a_{h\Psi_k^+ \Psi_l^+} (\mathcal{C}_R)_{ki} (\mathcal{C}_L)_{lj}, & b_{hX_i^+ X_j^+} &= b_{h\Psi_k^+ \Psi_l^+} (\mathcal{C}_L)_{ki}^* (\mathcal{C}_R)_{lj}^*, \\
 a_{G^0 X_i^+ X_j^+} &= a_{G^0 \Psi_k^+ \Psi_l^+} (\mathcal{C}_R)_{ki} (\mathcal{C}_L)_{lj}, & b_{G^0 X_i^+ X_j^+} &= b_{G^0 \Psi_k^+ \Psi_l^+} (\mathcal{C}_L)_{ki}^* (\mathcal{C}_R)_{lj}^*, \\
 a_{G^\pm X_i^+ X_j^0} &= a_{G^\pm \Psi_k^+ \Psi_l^0} (\mathcal{C}_R)_{ki} \mathcal{N}_{lj}, & b_{G^\pm X_i^+ X_j^0} &= b_{G^\pm \Psi_k^+ \Psi_l^0} (\mathcal{C}_L)_{ki}^* \mathcal{N}_{lj}^*, \\
 a_{G^\pm X_{++} X_i^+} &= a_{G^\pm X_{++} \Psi_j^+} (\mathcal{C}_L)_{ji}, & b_{G^\pm X_{++} X_i^+} &= b_{G^\pm X_{++} \Psi_j^+} (\mathcal{C}_R)_{ji}^*. \tag{A.17}
 \end{aligned}$$

## B Self energies

In this appendix, we give useful expressions for the self-energies of  $\chi_i^0$ ,  $\chi_i^\pm$ ,  $\chi^{\pm\pm}$ ,  $\gamma$ ,  $Z$ , and  $W$ , used for both the calculation of the mass corrections for dark sector fermions and the electroweak oblique parameters. In these calculations, we use the one-loop integrals whose definitions are consistent with ref. [23]:

$$A_0(m^2) = \frac{(2\pi\mu)^{4-D}}{i\pi^2} \int d^D q \frac{1}{q^2 - m^2 + i\varepsilon}, \tag{B.1}$$

$$B_0(p^2, m_1^2, m_2^2) = \frac{(2\pi\mu)^{4-D}}{i\pi^2} \int d^D q \frac{1}{[q^2 - m_1^2 + i\varepsilon][(p+q)^2 - m_2^2 + i\varepsilon]}, \tag{B.2}$$

$$p_\mu B_1(p^2, m_1^2, m_2^2) = \frac{(2\pi\mu)^{4-D}}{i\pi^2} \int d^D q \frac{q_\mu}{[q^2 - m_1^2 + i\varepsilon][(p+q)^2 - m_2^2 + i\varepsilon]}, \tag{B.3}$$

$$\begin{aligned}
 &g_{\mu\nu} B_{00}(p^2, m_1^2, m_2^2) + p_\mu p_\nu B_{11}(p^2, m_1^2, m_2^2) \\
 &= \frac{(2\pi\mu)^{4-D}}{i\pi^2} \int d^D q \frac{q_\mu q_\nu}{[q^2 - m_1^2 + i\varepsilon][(p+q)^2 - m_2^2 + i\varepsilon]}. \tag{B.4}
 \end{aligned}$$

We calculate the self-energies of  $\chi_i^0$ ,  $\chi_i^\pm$ , and  $\chi^{\pm\pm}$  in the  $\overline{\text{DR}}$  scheme with the 't Hooft-Feynman gauge, as in ref. [42]. At NLO, the  $\chi_i^0$ - $\chi_k^0$  self-energy has contributions from loops

of  $W^\pm \chi_j^\mp$ ,  $G^\pm \chi_j^\mp$ ,  $h \chi_j^0$ ,  $Z \chi_j^0$ , and  $G^0 \chi_j^0$ . We have

$$\begin{aligned}
 & 16\pi^2 \Sigma_{X_i^0 X_k^0}^{LV}(p^2) \\
 &= \sum_j \left( -2a_{WX_j^+ X_i^0}^* a_{WX_j^+ X_k^0} - 2b_{WX_j^+ X_i^0} b_{WX_j^+ X_k^0}^* - a_{G^\pm X_j^+ X_i^0}^* a_{G^\pm X_j^+ X_k^0} \right. \\
 &\quad \left. - b_{G^\pm X_j^+ X_i^0} b_{G^\pm X_j^+ X_k^0}^* \right) B_1(p^2, m_{\chi_j^\pm}^2, m_W^2) - \sum_j b_{hX_i^0 X_j^0} a_{hX_j^0 X_k^0} B_1(p^2, m_{\chi_j^0}^2, m_h^2) \\
 &\quad + \sum_j \left( -2a_{ZX_i^0 X_j^0} a_{ZX_j^0 X_k^0} - b_{G^0 X_i^0 X_j^0} a_{G^0 X_j^0 X_k^0} \right) B_1(p^2, m_{\chi_j^0}^2, m_Z^2), \tag{B.5}
 \end{aligned}$$

$$\begin{aligned}
 & 16\pi^2 \Sigma_{X_i^0 X_k^0}^{LS}(p^2) \\
 &= \sum_j \left( -4b_{WX_j^+ X_i^0}^* a_{WX_j^+ X_k^0} - 4a_{WX_j^+ X_i^0} b_{WX_j^+ X_k^0}^* + b_{G^\pm X_j^+ X_i^0}^* a_{G^\pm X_j^+ X_k^0} \right. \\
 &\quad \left. + a_{G^\pm X_j^+ X_i^0} b_{G^\pm X_j^+ X_k^0}^* \right) m_{\chi_j^\pm} B_0(p^2, m_{\chi_j^\pm}^2, m_W^2) + \sum_j a_{hX_i^0 X_j^0} a_{hX_j^0 X_k^0} m_{\chi_j^0} B_0(p^2, m_{\chi_j^0}^2, m_h^2) \\
 &\quad + \sum_j \left( -4b_{ZX_i^0 X_j^0} a_{ZX_j^0 X_k^0} + a_{G^0 X_i^0 X_j^0} a_{G^0 X_j^0 X_k^0} \right) m_{\chi_j^0} B_0(p^2, m_{\chi_j^0}^2, m_Z^2). \tag{B.6}
 \end{aligned}$$

The  $\chi_i^+ - \chi_k^+$  self-energy has contributions from loops of  $W^+ \chi_j^0$ ,  $G^+ \chi_j^0$ ,  $Z \chi_j^+$ ,  $G^0 \chi_j^+$ ,  $A \chi_j^+$ ,  $h \chi_j^+$ ,  $W^- \chi^{++}$ , and  $G^- \chi^{++}$ . Therefore,

$$\begin{aligned}
 & 16\pi^2 \Sigma_{X_i^+ X_k^+}^{LV}(p^2) \\
 &= \sum_j \left( -2a_{WX_i^+ X_j^0} a_{WX_k^+ X_j^0}^* - b_{G^\pm X_i^+ X_j^0} b_{G^\pm X_k^+ X_j^0}^* \right) B_1(p^2, m_{\chi_j^0}^2, m_W^2) \\
 &\quad + \sum_j \left( -2a_{ZX_i^+ X_j^+} a_{ZX_k^+ X_j^+} - b_{G^0 X_i^+ X_j^+} a_{G^0 X_k^+ X_j^+} \right) B_1(p^2, m_{\chi_j^\pm}^2, m_Z^2) \\
 &\quad - 2 \sum_j a_{AX_i^+ X_j^+} a_{AX_k^+ X_j^+} B_1(p^2, m_{\chi_j^\pm}^2, 0) - \sum_j b_{hX_i^+ X_j^+} a_{hX_k^+ X_j^+} B_1(p^2, m_{\chi_j^\pm}^2, m_h^2) \\
 &\quad + \left( -2a_{WX^{++} X_i^+}^* a_{WX^{++} X_k^+} - a_{G^\pm X^{++} X_i^+}^* a_{G^\pm X^{++} X_k^+} \right) B_1(p^2, m_{\chi^{\pm\pm}}^2, m_W^2), \tag{B.7}
 \end{aligned}$$

$$\begin{aligned}
 & 16\pi^2 \Sigma_{X_i^+ X_k^+}^{LS}(p^2) \\
 &= \sum_j \left( -4b_{WX_i^+ X_j^0} a_{WX_k^+ X_j^0}^* + a_{G^\pm X_i^+ X_j^0} b_{G^\pm X_k^+ X_j^0}^* \right) m_{\chi_j^0} B_0(p^2, m_{\chi_j^0}^2, m_W^2) \\
 &\quad + \sum_j \left( -4b_{ZX_i^+ X_j^+} a_{ZX_k^+ X_j^+} + a_{G^0 X_i^+ X_j^+} a_{G^0 X_k^+ X_j^+} \right) m_{\chi_j^\pm} B_0(p^2, m_{\chi_j^\pm}^2, m_Z^2) \\
 &\quad - 4 \sum_j b_{AX_i^+ X_j^+} a_{AX_k^+ X_j^+} m_{\chi_j^\pm} B_0(p^2, m_{\chi_j^\pm}^2, 0) + \sum_j a_{hX_i^+ X_j^+} a_{hX_k^+ X_j^+} m_{\chi_j^\pm} B_0(p^2, m_{\chi_j^\pm}^2, m_h^2) \\
 &\quad + \left( -4b_{WX^{++} X_i^+}^* a_{WX^{++} X_k^+} + b_{G^\pm X^{++} X_i^+}^* a_{G^\pm X^{++} X_k^+} \right) m_{\chi^{\pm\pm}} B_0(p^2, m_{\chi^{\pm\pm}}^2, m_W^2). \tag{B.8}
 \end{aligned}$$

The self-energy of  $\chi^{++}$  receives contributions from loops of  $W^+\chi_i^+$ ,  $G^+\chi_i^+$ ,  $A\chi^{++}$ , and  $Z\chi^{++}$ , and thus

$$\begin{aligned}
 & 16\pi^2 \Sigma_{X^{++}X^{++}}^{\text{LV}}(p^2) \\
 &= \sum_i \left( -2|a_{WX^{++}X_i^+}|^2 - |b_{G^{\pm}X^{++}X_i^+}|^2 \right) B_1(p^2, m_{\chi_i^+}^2, m_W^2) \\
 &\quad - 2a_{AX^{++}X^{++}}^2 B_1(p^2, m_{\chi^{\pm\pm}}^2, 0) - 2a_{ZX^{++}X^{++}}^2 B_1(p^2, m_{\chi^{\pm\pm}}^2, m_Z^2), \tag{B.9}
 \end{aligned}$$

$$\begin{aligned}
 & 16\pi^2 \Sigma_{X^{++}X^{++}}^{\text{LS}}(p^2) \\
 &= \sum_i \left( -4b_{WX^{++}X_i^+} a_{WX^{++}X_i^+}^* + a_{G^{\pm}X^{++}X_i^+} b_{G^{\pm}X^{++}X_i^+}^* \right) m_{\chi_i^+} B_0(p^2, m_{\chi_i^+}^2, m_W^2) \\
 &\quad - 4b_{AX^{++}X^{++}} a_{AX^{++}X^{++}} m_{\chi^{\pm\pm}} B_0(p^2, m_{\chi^{\pm\pm}}^2, 0) \\
 &\quad - 4b_{ZX^{++}X^{++}} a_{ZX^{++}X^{++}} m_{\chi^{\pm\pm}} B_0(p^2, m_{\chi^{\pm\pm}}^2, m_Z^2). \tag{B.10}
 \end{aligned}$$

The expressions for  $\Sigma^{\text{RV}}(p^2)$  and  $\Sigma^{\text{RS}}(p^2)$  can be obtained from  $\Sigma^{\text{LV}}(p^2)$  and  $\Sigma^{\text{LS}}(p^2)$  through  $a \leftrightarrow b$ , respectively.

Below we give the extra contributions to the vacuum polarization amplitudes of electroweak gauge bosons from the triplet and quadruplets. The contribution to the  $Z$  boson vacuum polarization comes from loops of  $\chi_i^0\chi_j^0$ ,  $\chi_i^+\chi_j^-$ , and  $\chi^{++}\chi^{--}$ :

$$\begin{aligned}
 16\pi^2 \Delta\Pi_{ZZ}(p^2) &= \frac{1}{2} \sum_{ij} \left[ \left( a_{ZX_j^0X_i^0} a_{ZX_i^0X_j^0} + b_{ZX_j^0X_i^0} b_{ZX_i^0X_j^0} \right) J_1(p^2, m_{\chi_i^0}^2, m_{\chi_j^0}^2) \right. \\
 &\quad \left. - 2 \left( a_{ZX_j^0X_i^0} b_{ZX_i^0X_j^0} + b_{ZX_j^0X_i^0} a_{ZX_i^0X_j^0} \right) m_{\chi_i^0} m_{\chi_j^0} B_0(p^2, m_{\chi_i^0}^2, m_{\chi_j^0}^2) \right] \\
 &\quad + \sum_{ij} \left[ \left( a_{ZX_j^+X_i^+} a_{ZX_i^+X_j^+} + b_{ZX_j^+X_i^+} b_{ZX_i^+X_j^+} \right) J_1(p^2, m_{\chi_i^{\pm}}^2, m_{\chi_j^{\pm}}^2) \right. \\
 &\quad \left. - 2 \left( a_{ZX_j^+X_i^+} b_{ZX_i^+X_j^+} + b_{ZX_j^+X_i^+} a_{ZX_i^+X_j^+} \right) m_{\chi_i^{\pm}} m_{\chi_j^{\pm}} B_0(p^2, m_{\chi_i^{\pm}}^2, m_{\chi_j^{\pm}}^2) \right] \\
 &\quad + \frac{g^2(3c_W^2 - s_W^2)^2}{2c_W^2} J_2(p^2, m_{\chi^{\pm\pm}}^2), \tag{B.11}
 \end{aligned}$$

where

$$\begin{aligned}
 J_1(p^2, m_1^2, m_2^2) &\equiv A_0(m_1^2) + A_0(m_2^2) - (p^2 - m_1^2 - m_2^2) B_0(p^2, m_1^2, m_2^2) - 4B_{00}(p^2, m_1^2, m_2^2), \\
 J_2(p^2, m^2) &\equiv 2A_0(m^2) - p^2 B_0(p^2, m^2, m^2) - 4B_{00}(p^2, m^2, m^2). \tag{B.12}
 \end{aligned}$$

The contribution to the  $W^+$  boson vacuum polarization comes from loops of  $\chi_i^0\chi_j^+$  and  $\chi_i^-\chi^{++}$ :

$$\begin{aligned}
 & 16\pi^2 \Delta\Pi_{WW}(p^2) \tag{B.13} \\
 &= \sum_{ij} \left[ \left( |a_{WX_j^+X_i^0}|^2 + |b_{WX_j^+X_i^0}|^2 \right) J_1(p^2, m_{\chi_i^0}^2, m_{\chi_j^+}^2) \right. \\
 &\quad \left. - 2 \left( a_{WX_j^+X_i^0} b_{WX_j^+X_i^0}^* + b_{WX_j^+X_i^0} a_{WX_j^+X_i^0}^* \right) m_{\chi_i^0} m_{\chi_j^+} B_0(p^2, m_{\chi_i^0}^2, m_{\chi_j^+}^2) \right] \\
 &\quad + \sum_i \left[ \left( |a_{WX^{++}X_i^+}|^2 + |b_{WX^{++}X_i^+}|^2 \right) J_1(p^2, m_{\chi_i^{\pm}}^2, m_{\chi^{\pm\pm}}^2) \right. \\
 &\quad \left. - 2 \left( a_{WX^{++}X_i^+} b_{WX^{++}X_i^+}^* + b_{WX^{++}X_i^+} a_{WX^{++}X_i^+}^* \right) m_{\chi_i^{\pm}} m_{\chi^{\pm\pm}} B_0(p^2, m_{\chi_i^{\pm}}^2, m_{\chi^{\pm\pm}}^2) \right].
 \end{aligned}$$

The contribution to the photon vacuum polarization comes from loops of  $\chi_i^+\chi_i^-$  and  $\chi^{++}\chi^{--}$ :

$$16\pi^2\Delta\Pi_{AA}(p^2) = 2e^2 \sum_i J_2(p^2, m_{\chi_i^\pm}^2) + 8e^2 J_2(p^2, m_{\chi^{\pm\pm}}^2). \quad (\text{B.14})$$

And finally, the contribution to the mixed photon-Z vacuum polarization also arises from loops of  $\chi_i^+\chi_i^-$  and  $\chi^{++}\chi^{--}$ :

$$16\pi^2\Delta\Pi_{ZA}(p^2) = e \sum_i (a_{Z\chi_i^+\chi_i^+} + b_{Z\chi_i^+\chi_i^+}) J_2(p^2, m_{\chi_i^\pm}^2) + \frac{2eg(3c_W^2 - s_W^2)}{c_W} J_2(p^2, m_{\chi^{\pm\pm}}^2). \quad (\text{B.15})$$

**Open Access.** This article is distributed under the terms of the Creative Commons Attribution License ([CC-BY 4.0](https://creativecommons.org/licenses/by/4.0/)), which permits any use, distribution and reproduction in any medium, provided the original author(s) and source are credited.

## References

- [1] ATLAS collaboration, *Observation of a new particle in the search for the Standard Model Higgs boson with the ATLAS detector at the LHC*, *Phys. Lett. B* **716** (2012) 1 [[arXiv:1207.7214](https://arxiv.org/abs/1207.7214)] [[INSPIRE](#)].
- [2] CMS collaboration, *Observation of a new boson at a mass of 125 GeV with the CMS experiment at the LHC*, *Phys. Lett. B* **716** (2012) 30 [[arXiv:1207.7235](https://arxiv.org/abs/1207.7235)] [[INSPIRE](#)].
- [3] G. Jungman, M. Kamionkowski and K. Griest, *Supersymmetric dark matter*, *Phys. Rept.* **267** (1996) 195 [[hep-ph/9506380](https://arxiv.org/abs/hep-ph/9506380)] [[INSPIRE](#)].
- [4] G. Bertone, D. Hooper and J. Silk, *Particle dark matter: Evidence, candidates and constraints*, *Phys. Rept.* **405** (2005) 279 [[hep-ph/0404175](https://arxiv.org/abs/hep-ph/0404175)] [[INSPIRE](#)].
- [5] J.L. Feng, *Dark Matter Candidates from Particle Physics and Methods of Detection*, *Ann. Rev. Astron. Astrophys.* **48** (2010) 495 [[arXiv:1003.0904](https://arxiv.org/abs/1003.0904)] [[INSPIRE](#)].
- [6] H. Goldberg, *Constraint on the Photino Mass from Cosmology*, *Phys. Rev. Lett.* **50** (1983) 1419 [*Erratum ibid.* **103** (2009) 099905] [[INSPIRE](#)].
- [7] J.R. Ellis, J.S. Hagelin, D.V. Nanopoulos, K.A. Olive and M. Srednicki, *Supersymmetric Relics from the Big Bang*, *Nucl. Phys. B* **238** (1984) 453 [[INSPIRE](#)].
- [8] G. Servant and T.M.P. Tait, *Is the lightest Kaluza-Klein particle a viable dark matter candidate?*, *Nucl. Phys. B* **650** (2003) 391 [[hep-ph/0206071](https://arxiv.org/abs/hep-ph/0206071)] [[INSPIRE](#)].
- [9] H.-C. Cheng, J.L. Feng and K.T. Matchev, *Kaluza-Klein dark matter*, *Phys. Rev. Lett.* **89** (2002) 211301 [[hep-ph/0207125](https://arxiv.org/abs/hep-ph/0207125)] [[INSPIRE](#)].
- [10] M. Cirelli, N. Fornengo and A. Strumia, *Minimal dark matter*, *Nucl. Phys. B* **753** (2006) 178 [[hep-ph/0512090](https://arxiv.org/abs/hep-ph/0512090)] [[INSPIRE](#)].
- [11] R. Essig, *Direct Detection of Non-Chiral Dark Matter*, *Phys. Rev. D* **78** (2008) 015004 [[arXiv:0710.1668](https://arxiv.org/abs/0710.1668)] [[INSPIRE](#)].
- [12] R. Mahbubani and L. Senatore, *The minimal model for dark matter and unification*, *Phys. Rev. D* **73** (2006) 043510 [[hep-ph/0510064](https://arxiv.org/abs/hep-ph/0510064)] [[INSPIRE](#)].

- [13] F. D’Eramo, *Dark matter and Higgs boson physics*, *Phys. Rev. D* **76** (2007) 083522 [[arXiv:0705.4493](#)] [[INSPIRE](#)].
- [14] R. Enberg, P.J. Fox, L.J. Hall, A.Y. Papaioannou and M. Papucci, *LHC and dark matter signals of improved naturalness*, *JHEP* **11** (2007) 014 [[arXiv:0706.0918](#)] [[INSPIRE](#)].
- [15] T. Cohen, J. Kearney, A. Pierce and D. Tucker-Smith, *Singlet-Doublet Dark Matter*, *Phys. Rev. D* **85** (2012) 075003 [[arXiv:1109.2604](#)] [[INSPIRE](#)].
- [16] L. Calibbi, A. Mariotti and P. Tziveloglou, *Singlet-Doublet Model: Dark matter searches and LHC constraints*, *JHEP* **10** (2015) 116 [[arXiv:1505.03867](#)] [[INSPIRE](#)].
- [17] A. Freitas, S. Westhoff and J. Zupan, *Integrating in the Higgs Portal to Fermion Dark Matter*, *JHEP* **09** (2015) 015 [[arXiv:1506.04149](#)] [[INSPIRE](#)].
- [18] A. Dedes and D. Karamitros, *Doublet-Triplet Fermionic Dark Matter*, *Phys. Rev. D* **89** (2014) 115002 [[arXiv:1403.7744](#)] [[INSPIRE](#)].
- [19] H. Georgi, *Lie algebras in particle physics. From isospin to unified theories*, *Front. Phys.* **54** (1982) 1 [[INSPIRE](#)].
- [20] J.L. Feng, T. Moroi, L. Randall, M. Strassler and S.-f. Su, *Discovering supersymmetry at the Tevatron in wino LSP scenarios*, *Phys. Rev. Lett.* **83** (1999) 1731 [[hep-ph/9904250](#)] [[INSPIRE](#)].
- [21] R.J. Hill and M.P. Solon, *Universal behavior in the scattering of heavy, weakly interacting dark matter on nuclear targets*, *Phys. Lett. B* **707** (2012) 539 [[arXiv:1111.0016](#)] [[INSPIRE](#)].
- [22] N. Baro and F. Boudjema, *Automatised full one-loop renormalisation of the MSSM II: The chargino-neutralino sector, the sfermion sector and some applications*, *Phys. Rev. D* **80** (2009) 076010 [[arXiv:0906.1665](#)] [[INSPIRE](#)].
- [23] A. Denner, *Techniques for calculation of electroweak radiative corrections at the one loop level and results for W physics at LEP-200*, *Fortsch. Phys.* **41** (1993) 307 [[arXiv:0709.1075](#)] [[INSPIRE](#)].
- [24] T. Fritzsche and W. Hollik, *Complete one loop corrections to the mass spectrum of charginos and neutralinos in the MSSM*, *Eur. Phys. J. C* **24** (2002) 619 [[hep-ph/0203159](#)] [[INSPIRE](#)].
- [25] T. Hahn and M. Pérez-Victoria, *Automatized one loop calculations in four-dimensions and D-dimensions*, *Comput. Phys. Commun.* **118** (1999) 153 [[hep-ph/9807565](#)] [[INSPIRE](#)].
- [26] PLANCK collaboration, P.A.R. Ade et al., *Planck 2015 results. XIII. Cosmological parameters*, [arXiv:1502.01589](#) [[INSPIRE](#)].
- [27] GFITTER GROUP collaboration, M. Baak et al., *The global electroweak fit at NNLO and prospects for the LHC and ILC*, *Eur. Phys. J. C* **74** (2014) 3046 [[arXiv:1407.3792](#)] [[INSPIRE](#)].
- [28] LUX collaboration, D.S. Akerib et al., *First results from the LUX dark matter experiment at the Sanford Underground Research Facility*, *Phys. Rev. Lett.* **112** (2014) 091303 [[arXiv:1310.8214](#)] [[INSPIRE](#)].
- [29] FERMI-LAT collaboration, M. Ackermann et al., *Searching for Dark Matter Annihilation from Milky Way Dwarf Spheroidal Galaxies with Six Years of Fermi Large Area Telescope Data*, *Phys. Rev. Lett.* **115** (2015) 231301 [[arXiv:1503.02641](#)] [[INSPIRE](#)].
- [30] K. Griest and D. Seckel, *Three exceptions in the calculation of relic abundances*, *Phys. Rev. D* **43** (1991) 3191 [[INSPIRE](#)].

- [31] A. Alloul, N.D. Christensen, C. Degrande, C. Duhr and B. Fuks, *FeynRules 2.0 — A complete toolbox for tree-level phenomenology*, *Comput. Phys. Commun.* **185** (2014) 2250 [[arXiv:1310.1921](#)] [[INSPIRE](#)].
- [32] M. Backovic, K. Kong and M. McCaskey, *MadDM v.1.0: Computation of Dark Matter Relic Abundance Using MadGraph5*, *Physics of the Dark Universe* **5-6** (2014) 18 [[arXiv:1308.4955](#)] [[INSPIRE](#)].
- [33] J. Alwall et al., *The automated computation of tree-level and next-to-leading order differential cross sections and their matching to parton shower simulations*, *JHEP* **07** (2014) 079 [[arXiv:1405.0301](#)] [[INSPIRE](#)].
- [34] M.E. Peskin and T. Takeuchi, *A new constraint on a strongly interacting Higgs sector*, *Phys. Rev. Lett.* **65** (1990) 964 [[INSPIRE](#)].
- [35] M.E. Peskin and T. Takeuchi, *Estimation of oblique electroweak corrections*, *Phys. Rev. D* **46** (1992) 381 [[INSPIRE](#)].
- [36] J.R. Ellis, A. Ferstl and K.A. Olive, *Reevaluation of the elastic scattering of supersymmetric dark matter*, *Phys. Lett. B* **481** (2000) 304 [[hep-ph/0001005](#)] [[INSPIRE](#)].
- [37] HERMES collaboration, A. Airapetian et al., *Precise determination of the spin structure function  $g_1$  of the proton, deuteron and neutron*, *Phys. Rev. D* **75** (2007) 012007 [[hep-ex/0609039](#)] [[INSPIRE](#)].
- [38] S. Profumo, W. Shepherd and T. Tait, *Pitfalls of dark matter crossing symmetries*, *Phys. Rev. D* **88** (2013) 056018 [[arXiv:1307.6277](#)] [[INSPIRE](#)].
- [39] S. Dawson et al., *Working Group Report: Higgs Boson*, [arXiv:1310.8361](#) [[INSPIRE](#)].
- [40] M. Low and L.-T. Wang, *Neutralino dark matter at 14 TeV and 100 TeV*, *JHEP* **08** (2014) 161 [[arXiv:1404.0682](#)] [[INSPIRE](#)].
- [41] J. Bramante et al., *Relic neutralino surface at a 100 TeV collider*, *Phys. Rev. D* **91** (2015) 054015 [[arXiv:1412.4789](#)] [[INSPIRE](#)].
- [42] D.M. Pierce, J.A. Bagger, K.T. Matchev and R.-j. Zhang, *Precision corrections in the minimal supersymmetric standard model*, *Nucl. Phys. B* **491** (1997) 3 [[hep-ph/9606211](#)] [[INSPIRE](#)].